SUPPLEMENTARY MATERIAL

Expanded Methods and Results

1. Patients, study cohorts, and curation strategies for genetic variations

1) BrS cohort-I

BrS cohort-I consisted of 415 Japanese probands with BrS who underwent genetic testing for *SCN5A* mutations and followed up between 1988 and 2013.[1] Genomic PCR followed by Sanger sequencing identified 55 rare *SCN5A* variants in 60 probands (*SCN5A*(+)), which were categorized as missense (n=39), in-frame deletion (n=1), nonsense (n=6), frame-shift truncation (n=6), and canonical splice site variations (n=3) (Table S1). Their pathogenesis was curated based on several human variation databases and seven *in silico* phenotype prediction algorithms (SIFT, PolyPhen-2, Species, Paralogue, Grantham, Condel, MutationAssesor) as originally described by Kapplinger et al.[2] The scores of seven algorithms for each mutation are listed in Table S4.

In our study, we first re-evaluated the frequency of all 55 variations using two global human variation databases (gnomAD,[3] 1000 Genomes Project[4]) and the Japanese whole-genome sequencing database (4.7KJPN).[5] Nonsense, frame-shift truncation, and canonical splice site variations (n=15) were classified as null variants of pathogenicity with very strong evidence (PVS1) according to the ACMG-AMP guidelines.[6] We then performed a PubMed search for previous literature describing functional characterizations of the 55 variations and found 21 publications (including five of our own) describing the loss-of-function (LOF) properties of 17 missense, one in-frame deletion, and four nonsense variations. Based on these database searches, 22 missense variations were assigned as variants of unknown significance (VUSs) (Figure 1, Table S1), and they were subjected to functional analyses using patch clamp (Figure S1).

In order to identify mutations in genes other than *SCN5A*, whole-exome sequence was required. However, the cohort-I patients only agreed to the genetic testing for *SCN5A* mutations at the time of enrollment, and some of them have already passed away; therefore, we freshly recruited independent Japanese BrS probands to perform whole-exome sequencing.

2) BrS cohort-II

In order to identify non-*SCN5A* genes associated with lethal arrhythmic events in BrS, we enrolled new unrelated BrS patients (originally n=297) who had been diagnosed as "*SCN5A* mutation-negative" in advance by genetic testing in clinical institutions all over Japan. After performing whole-exome sequencing in BrS-probands and control Japanese (n=372) in our study and found 9 *SCN5A* mutation carriers whose mutations were overlooked during the initial Sanger sequencings in each institution. Accordingly, we excluded 9 patients from the new BrS cohort leaving 288 probands in the Japanese *SCN5A* mutation-negative BrS (BrS cohort-II).

Genetic testing of BrS in Japan is performed preferentially for patients with symptoms or lethal arrhythmic events, therefore, symptoms and the history of lethal arrhythmic events of cohort-II were more prevalent than in cohort-I (Table 1).

2. Electrophysiological analysis of 22 *SCN5A*-VUSs

Functionally undetermined 22 VUSs listed in table S1 were subjects for the electrophysiological analysis by patch-clamping in this study. Plasmids with these 22 VUSs were created by site-directed mutagenesis using the QuikChange site-directed mutagenesis kit (Agilent Technologies, Santa Clara, CA) and specific primers on wild-type (WT) *SCN5A* plasmid encoding human Nav1.5 (NM_000335.5). Absence of unwanted sequence errors was confirmed by Sanger sequencing.

Patch-clamp analysis for *SCN5A* mutations were performed as previously described.[7] Briefly, mammalian cell line HEK293T (i.e. tsA-201) ($4x10^5$) was passaged on 6 cm dishes, and 24 hrs later, transiently transfected with pEGFP plasmids (0.8 μg) and WT or mutant *SCN5A* plasmids Nav1.5 (1.6 μg) using Lipofectamine LTX (Thermo Fisher Scientific, Waltham, MA). Another 24 hrs later, cells were subjected to the patch-clamp analysis. Whole-cell I_{Na} currents and capacitances were recorded from the cells labelled with EGFP fluorescence using Axopatch 200B amplifier (Molecular devices, Sunnyvale, CA). Series resistance errors were reduced by 60~70% using electronic compensation. Holding potentials were set at -120 mV, and pipette resistance was 2-3 MΩ. Bath solutions for I_{Na} recordings contained (in mmol/L): 36 NaCl, 109 N-methylglucamine, 4 KCl, 1.8 $CaCl_2$, 1 $MgCl_2$, 10 HEPES and 10 glucose, with a pH of 7.35 adjusted with NaOH. Pipette solution for I_{Na} recordings contained (in mmol/L): 10 NaF, 110 CsF, 20 CsCl, 10 EGTA, and 10 HEPES with a pH of 7.35 adjusted with CsOH. All signals were acquired at 20-50 kHz (Digidata 1332, Molecular devices) with Clampex 10 software (Molecular devices) and filtered at 5 kHz with a 4-pole Bessel low pass filter. Membrane currents were analyzed with Clampfit 10 software (Molecular devices) and SigmaPlot (Systat Software Inc, CA).

Current-voltage relationship and voltage-dependent activation were determined by the test pulse stepped to a voltage between -90 mV to +70 mV for 20 ms. Peak Na current density (peak current amplitude/cell capacitance; pA/pF) of each mutation was calculated, and the % peak current density is a fraction of peak current density of mutant Na1.5 against WT-Nav1.5. For assessment of steady-state inactivation, the membrane potential was stepped to a voltage between -140 and -30 mV for 100 ms, and then peak Na current was measured during a -20 mV test potential. Recovery from inactivation was assessed by a double-pulse protocol consisting of a 500 ms prepulse to -20 mV, which was designed to fully inactivate all channels, followed by a variable-duration interpulse interval (Δt) at -120 mV and a test pulse to -20 mV. The time from establishing the whole-cell configuration to the onset of recording was consistent cell-to-cell to exclude the possible time-dependent shift of steady-state inactivation. To determine activation parameters, the current-voltage relationship was fitted to the Boltzmann equation: $I= (V-V_{rev}) \times G_{max} \times[1+\exp(V-V_{1/2})/k]^{-1}$, where I is the peak Na current during the test pulse potential V. The parameters estimated by the fitting are V_{rev} (reversal potential), G_{max} (maximum conductance), $V_{1/2}$ (voltage for half-activation), and k (slope factor). Steady-state inactivation was fitted with the Boltzmann equation: $I/I_{max} = [1 + \exp((V - V_{1/2})/k)]^{-1}$ to determine the membrane potential for half maximal inactivation ($V_{1/2}$) and the slope factor k. Recovery from inactivation was analyzed by fitting data with a double exponential equation: $I/I_{max}= A_0 + A_{fast} \times \exp(-t/\tau_{fast}) + A_{slow} \times \exp(-t/\tau_{slow})$, where I_{max} is the maximum peak Na current, A_0 is a constant value, A_{fast} and A_{slow} are fractions of fast and slow recovering components, respectively,

and τ_{fast} and τ_{slow} are the time constants of fast and slow recovering components, respectively. One-way ANOVA followed by post hoc Bonferroni correction was used to statistically analyze the channel properties among multiple groups.

The original patch clamp data of the p.N406S were provided by Itoh et al.[8] and re-analyzed. The %peak current density of p.N406S was 81.6±51.2 (n=20, p=0.153 vs WT), and it was assigned to non-LOF.

3. Evaluation of channel properties for predicting the lethal arrhythmic events

Three major Na channel properties of the patch clamp data; activation (shift of $V_{1/2}$), inactivation (shift of $V_{1/2}$), and %peak current density, were used for univariate analysis using a Cox proportional hazards model in 28 functional *SCN5A* variants (L136P, R282H, R376H, N406S, Y416C, E428K, R689H, R693C, A735V, Q779K, R814Q, R988Q, R1195H, H1200Y, E1225K, T1247I, V1328M, V1405M, A1428S, R1432S, K1527R, R1644C, R1644H, T1709M, E1784K, R1913C, R1919H, H1923D; Tables S2, S4). Receiver operating characteristic analysis showed significant association (p=0.01) between %peak current density and lethal arrhythmic events [area under the curve (AUC)=0.73 (95% CI: 0.56-0.91), cut-off values 66.0%]. The optimal cut-off value 66.0% was very close to the %peak current density border zone between LOF variants group and non-LOF group (62.0%-65.6%, between A1428S and R988Q of the Figure 2). No significant relationships were seen with activation [AUC=0.54 (95%CI: 0.20-0.72), p=0.77, cut-off value=-2.5 mV] or inactivation parameters [AUC=0.60 (95%CI: 0.35-0.84), p=0.44, cut-off value=3.3 mV]. These data indicate that the %peak current density is the most accurate channel property to predict the lethal events in BrS. The border zone %peak current density of LOF variants and Non-LOF variants was 53.2% (R693C)-65.6% (R988Q) (Table S2).

4. Sensitivity analyses using bootstrap method

We performed bootstrap methods to obtain 95% confidence intervals (CIs) for the annual event rates (Table 2) and the hazard ratios (HRs) (Table 3). We performed the analysis using 500 bootstrap resamples and obtained 500 HRs using Cox proportional hazard models, of which the mean values were point-estimates, and the 2.5th and 97.5th percentiles were 95% CIs. R statistical software (version 4.0.2),[9] R package "boot",[10, 11] and R package "survival" were used.[12] Note that we used seed number "123". As shown in the Table S6A, bootstrapped annual event rates of all BrS patients, *in silico*-predicted pathogenic rare *SCN5A* variant carriers, and *in vitro*-validated LOF *SCN5A* mutation carriers were 2.5%/year (95%CI: 1.85–3.12), 5.1%/year (95%CI: 2.37–8.49), and 7.9%/year (95%CI: 3.99–14.60), respectively; compatible with the observation presented in Table 2. Bootstrapped HRs (95%CI) of the variables evaluated by univariate analysis (Table S6B) were comparable to those in Table 3A, except that the bootstrap method was not effective in calculating the HR of LAE by gender due to the small sample size of female patients (Male=403, Female=12). Multivariate analysis showed that the HR of LOF-*SCN5A* mutations (HR=2.98, 95%CI: 1.31–6.08) was higher than that of *in silico*-predicted rare *SCN5A* variations (HR=2.06, 95%CI: 1.004–4.16) (Table S6C), consistent with the data in Table 3B.

5. Whole-exome sequencing

Genomic DNA was extracted from peripheral blood lymphocytes of the Japanese probands of BrS cohort-II (n=288) and controls (n=372) by standard protocols. All the procedures of sequencings and data processing were performed as previously described.[13] The DNA yields were assessed by measurements using Qubit fluorometer (Thermo Fisher Scientific) and Quant-IT dsDNA Assay Kit, Broad Range (Thermo Fisher Scientific). The purity of the DNA was assessed by spectrophotometry (OD 260:280 and 260:230 ratios) using a Nanodrop instrument (Thermo Fisher Scientific). After obtaining sheared genomic DNA of the target base pair size by Covaris E220 (Covaris, Woburn, MA), individual sample libraries were prepared by using Agilent SureSelect Exome Target Enrichment System (V4: case=12; V5: control=127; V5+UTRs: control= 208; V6: case=276, control=37) (Agilent Technologies, Santa Clara, CA), and sequenced on the Hiseq2500 platform (Illumina, San Diego, CA) with paired-end reads of 101 bp for insert libraries consisting of 150 to 200 bp fragments. Acquired sequence data were converted into Fastq format by bcl2fastq software, and aligned and mapped to the human reference genome sequence hg19/GRCh37 by Novoalign software. (Novocraft Technologies, Kuala Lumpur, Malaysia) Aligned reads were sorted by Novosort software (Novocraft) and subjected to the marking of PCR and optical duplication by MarkDuplicates in the Picard tools package. Whole-exome data resulted in an average depth of 71 and a mean coverage of 95.4% at 10-fold. The Genome Analysis Toolkit (GATK) v3.3-0 was used to perform local realignment (GATK IndelRealigner) and variant call (GATK HaplotypeCaller) was implemented in an in-house workflow management tool. The candidate variations causing nonsynonymous, stop-gain, stop-loss or splice site substitutions and insertions/deletions (indels) occurring frameshift, in-frame or splice sites substitution were determined by using GATK. Single nucleotide variations (SNVs) and indels were annotated using ANNOVAR software. Substitutions that met the following criteria were selected as “deleterious”: (1) stop gain, stop loss, nonsynonymous, or splice site mutations according to GENCODE basic version 19 downloaded from the UCSC genome browser; (2) alternative allele frequencies at mutation loci ≤0.5% in the following databases: 1000 Genomes Project data on all populations[4]; the Genome Aggregation Database as ethnic matched databases (gnomAD)[3]; and SNV allele frequency collected from whole-genome sequencing data of 4,773 healthy Japanese individuals (4.7KJPN)[5]; and (3) mutations not included in the UCSC segmental duplication region. Variations with minor allele frequencies (MAF) >1% in any of the public databases (gnomAD, 1000 Genomes and 4.7KJPN) were filtered out.

6. Gene-wise association test

To identify novel genes predisposing to BrS, gene-wise association tests were carried out to compare the proportion of rare variations with MAF of less than 1.0%. After the collection of rare variations by whole-exome sequencings, we removed common variants using the following criteria: alternative allele frequency of more than 1.0% in any public databases (ExAC,[14] ESP6500,[15] 1000 Genomes,[4] HGVD,[16] and ToMMo 2KJPN[17]) or more than 1.0% in control samples in this study; call rate of less than 95% in the study samples;

and genotyping quality score of less than 99. We also removed variants not being any of nonsynonymous, stop-gain, stop-loss, frameshift, nor splicing-affected based on the GENCODE basic v19 gene prediction.[18] For a single-gene wise association test, three different statistical tests: Combined Multivariate and Collapsing (CMC),[19] Madsen-Browning method,[20] and SNP-set Kernel Association Test (SKAT-O),[21] which are implemented in Efficient and Parallelizable Association Container Toolbox (EPACTS version 3.3.0) (Figure S6).[22] CMC method was used to filter the genes as the burden test, while SKAT-O as the combined test of burden and variance component. For weighing variants, MAF of control subjects were used for the CMC and Madsen-Browning methods. Bonferroni adjustment was used for multiple testing resulting in a cutoff of $P<2.94\times10^{-6}$ (=0.05/16,985) as a gene-wise significant level.

7. Rare variants of *SCN5A*-modulating BrS-associated genes

Among previously recognised 22 non-*SCN5A* BrS-associated genes, rare variations (MAF<1% or 0.3%) were found in only 17 genes except 5 genes (*ABCC9, ANK2, CACNB2, KCNE5, FGF12*), but they were not enriched in BrS cohort-II (Table S7). Among the 17 non-*SCN5A* BrS-associated genes, we defined eight genes (*GPD1L, PKP2, MOG1*, *SCN10A*, *SCN1B*, *SCN2B*, *SCN3B*, and *SLMAP*) as *SCN5A*-modulating BrS-associated genes that are known to modulate cardiac Na channel function. We performed gene-wise rare variation association test, but rare variants of neither 17 BrS-associated genes nor 8 *SCN5A*-modifying BrS-associated genes were enriched in BrS cohort-II (Table S8). Kaplan-Meier analysis demonstrated that the rare variations of neither 17 BrS-associated genes nor 8 *SCN5A*-modifying BrS-associated genes affected the event-free survival (Figure 5, and Figure S7).

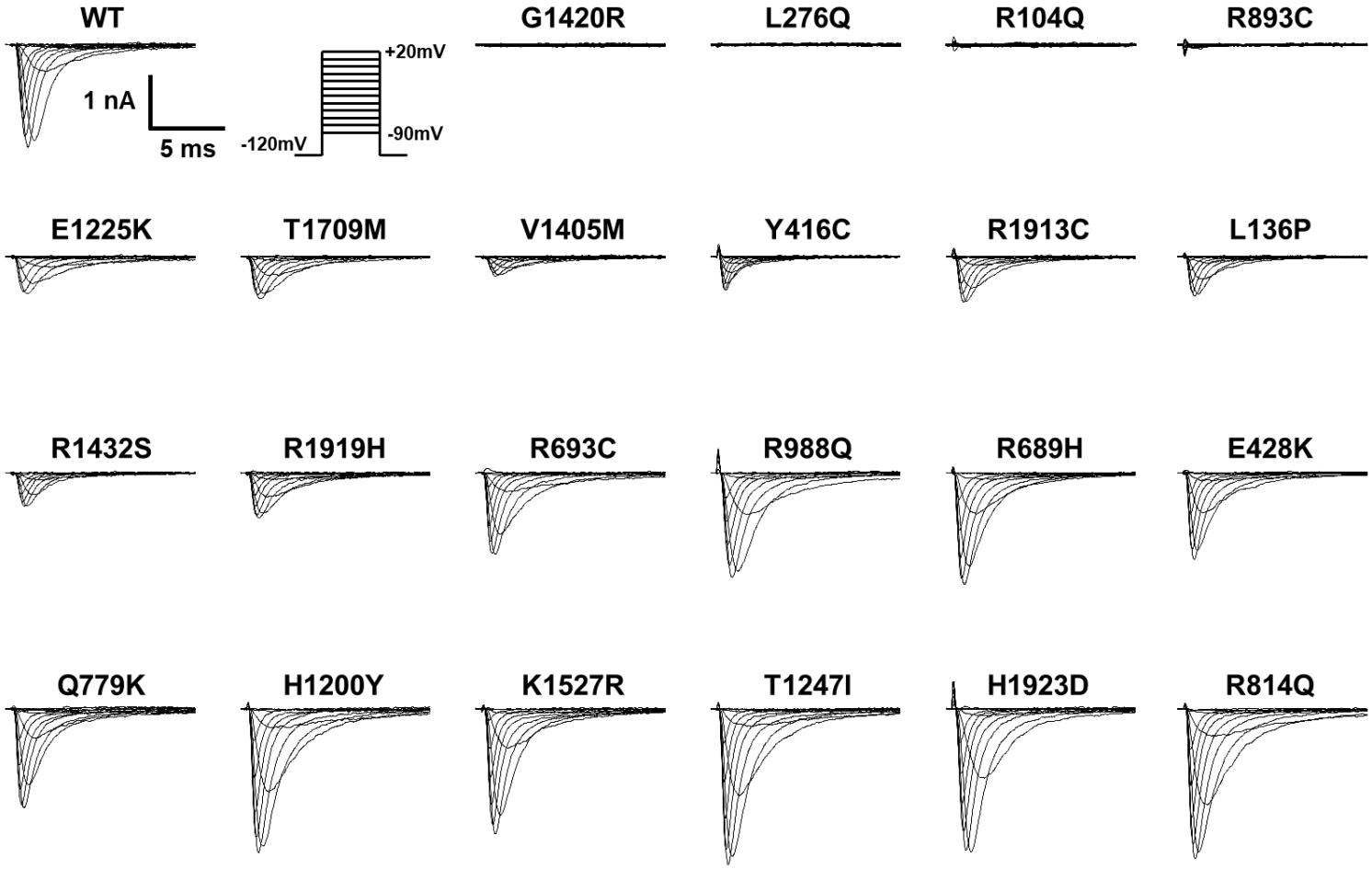

Figure S1. Representative current traces of WT and 22 missense VUS Nav1.5 channels heterologously expressed in HEK293T cells.
Whole-cell Na currents were recorded by the test pulses (from -90 mV to +20 mV with 10 mV increment) from a holding potential of -120 mV, and the peak current density (=peak current amplitude/cell capacitance) of each variant was calculated. Percentage peak current density, as a fraction of peak current density versus wild type (WT)-Nav1.5, was plotted in the Figure 2. Statistical analysis revealed significant reduction of peak current density than WT, i.e. loss-of-function (LOF) properties, in 13 variations (G1420R–R693C), but not in the other 9 variations (Non-LOF; R988Q–R814Q). Further electrophysiological data are available in the Table 2. The border zone %peak current density of LOF and Non-LOF was 53.2% (R693C)- 65.6% (R988Q).

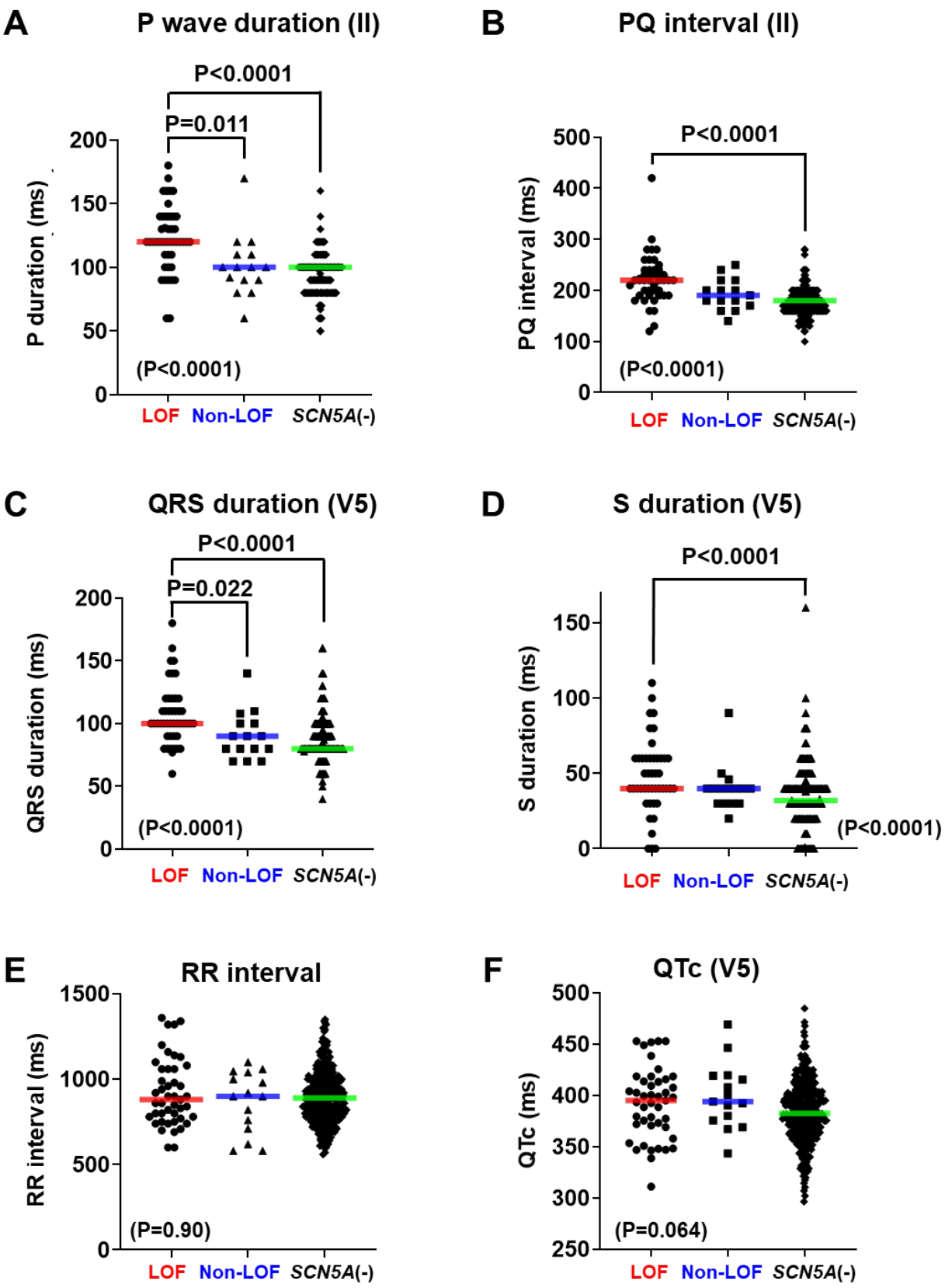

Figure S2. ECG parameters of patients with BrS of three subgroups classified by the Na channel function properties. A. P wave duration, **B**. PQ interval, **C**. QRS duration, **D**. S duration, **E**. RR-interval, and **F**. Corrected QT interval by Bazett's formula (QTc) of three groups are shown. Patients carrying the LOF-*SCN5A* mutations exhibited significantly impaired ECG conduction parameters compared with those with Non-LOF and/or *SCN5A* mutation non-carriers (*SCN5A*(-)). The horizontal bar represents the median. Statistical analysis was performed using Kruskal-Wallis test and post-hoc Dunn's test for multiple comparisons. P values with parentheses indicate statistical significance among three groups.

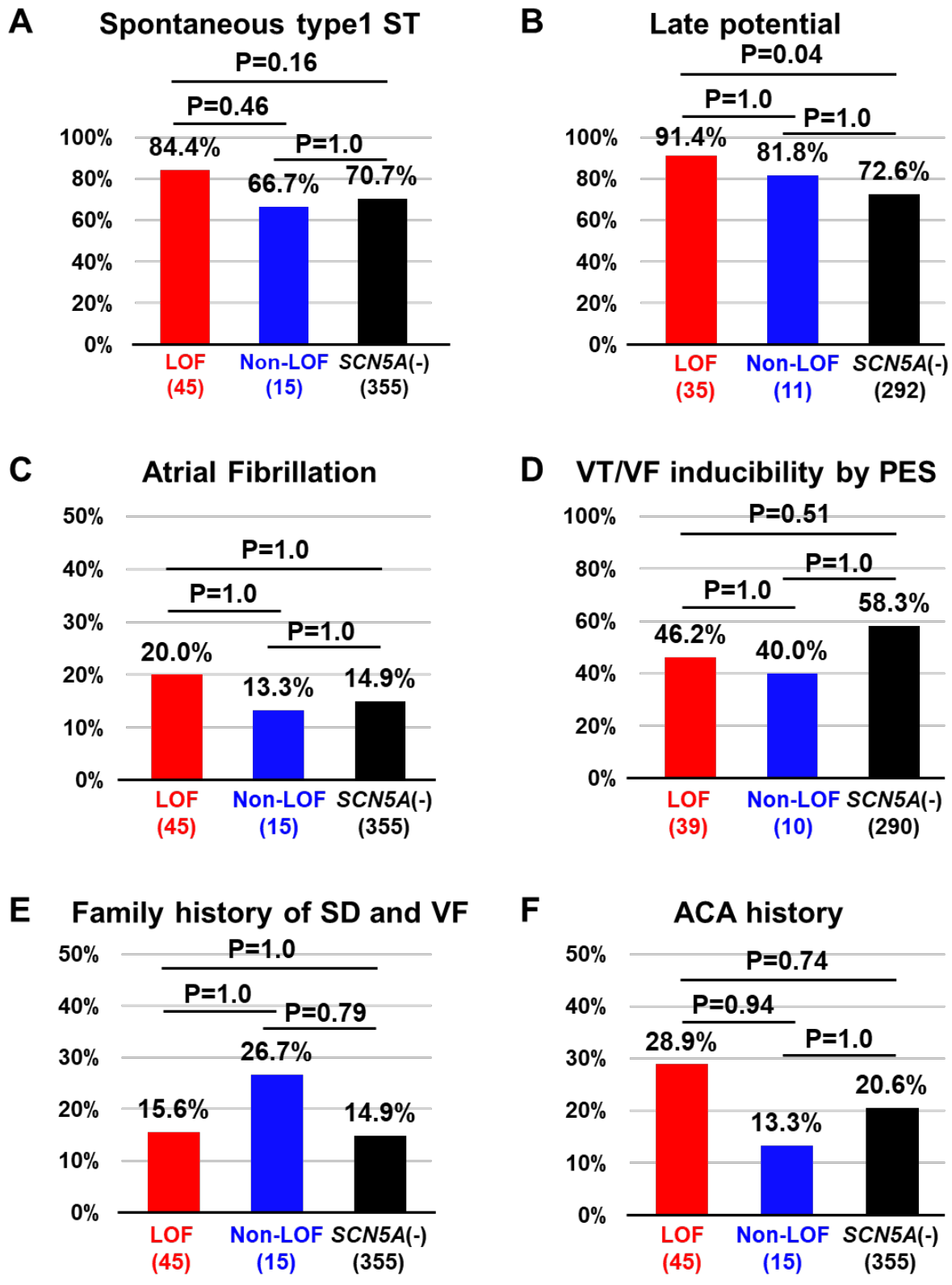

Figure S3. Electrophysiological and clinical findings among three groups of BrS cohort-I.
There were no significant differences among three groups in terms of **A**. spontaneous type-1 ST elevation, **C**. atrial fibrillation, **D.** VT/VF inducibility by programmed electrical stimulation (PES), **E**. Family history of sudden death and VF, and **F.** Aborted cardiac arrest (ACA) history. **B.** Late potential was more prevalent in LOF than in *SCN5A*(-). Statistical analysis was performed using Fisher's exact test with Bonferroni adjustment for multiple comparisons.

A

SCN5A status	LOF	Non-LOF	*SCN5A*(-)	Total
ICD discharge (+)	12	0	44	56
ICD discharge (-)	1	0	5	6

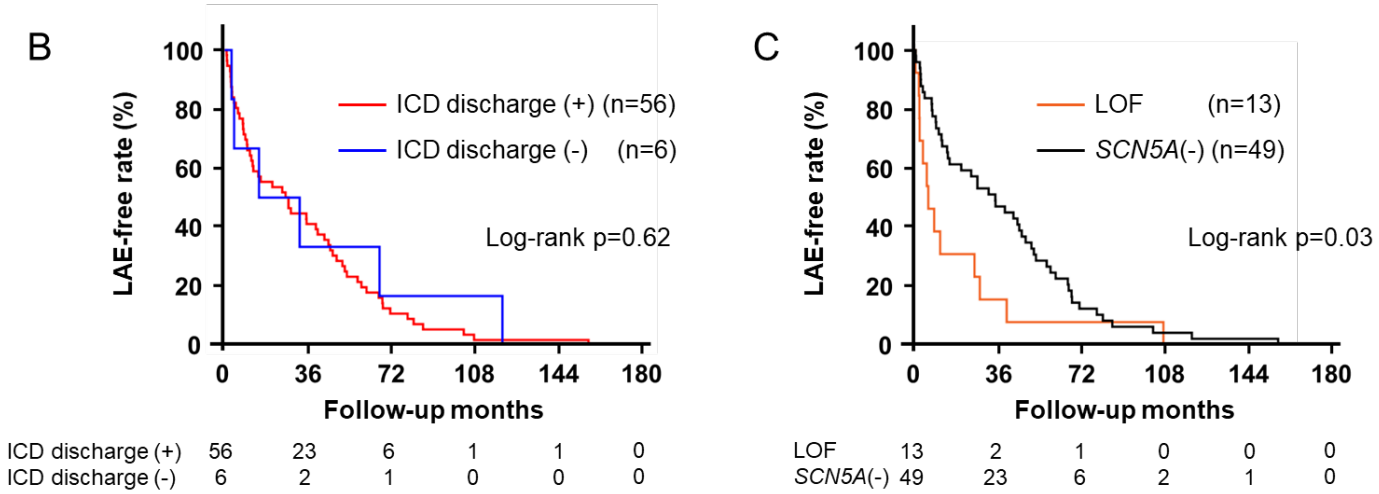

D. Estimated LAE-free period (months)

	Mean ± SE	95% CI
ICD discharge (+)	34.4 ± 4.4	25.7-43.0
ICD discharge (-)	40.1 ± 18.6	3.6-76.7

E. Estimated LAE-free period (months)

	Mean ± SE	95% CI
LOF	19.1 ± 8.1	3.2-35.0
SCN5A(-)	39.1 ± 4.9	29.5-48.7

Figure S4. *SCN5A* status and the Kaplan-Meier analysis of 62 probands experienced lethal arrhythmic events.
A. *SCN5A* status and the ICD discharges during the follow-up period of 62 probands. **B.** Kaplan-Meier analyses of lethal arrhythmic event (LAE)-free survival rate of 62 probands with (n=56) or without (n=6) appropriated ICD discharges showed nearly superimposable curves during the follow-up period (log-rank P=0.62). These data support the notion that an appropriate ICD discharge serves as a surrogate for sudden cardiac death in BrS. **C.** LOF-*SCN5A* carriers (n=13) experienced significantly earlier LAEs than *SCN5A*(-) (n=49), consistent with the findings in Fig 4C (log-rank P=0.03). **D, E**. Estimated LAE-free period of each group. Note that no probands carrying Non-LOF *SCN5A* variations experienced LAEs during the follow up. These data suggest that the prognosis of BrS patients can be discriminated based on LOF properties of the *SCN5A* variants.

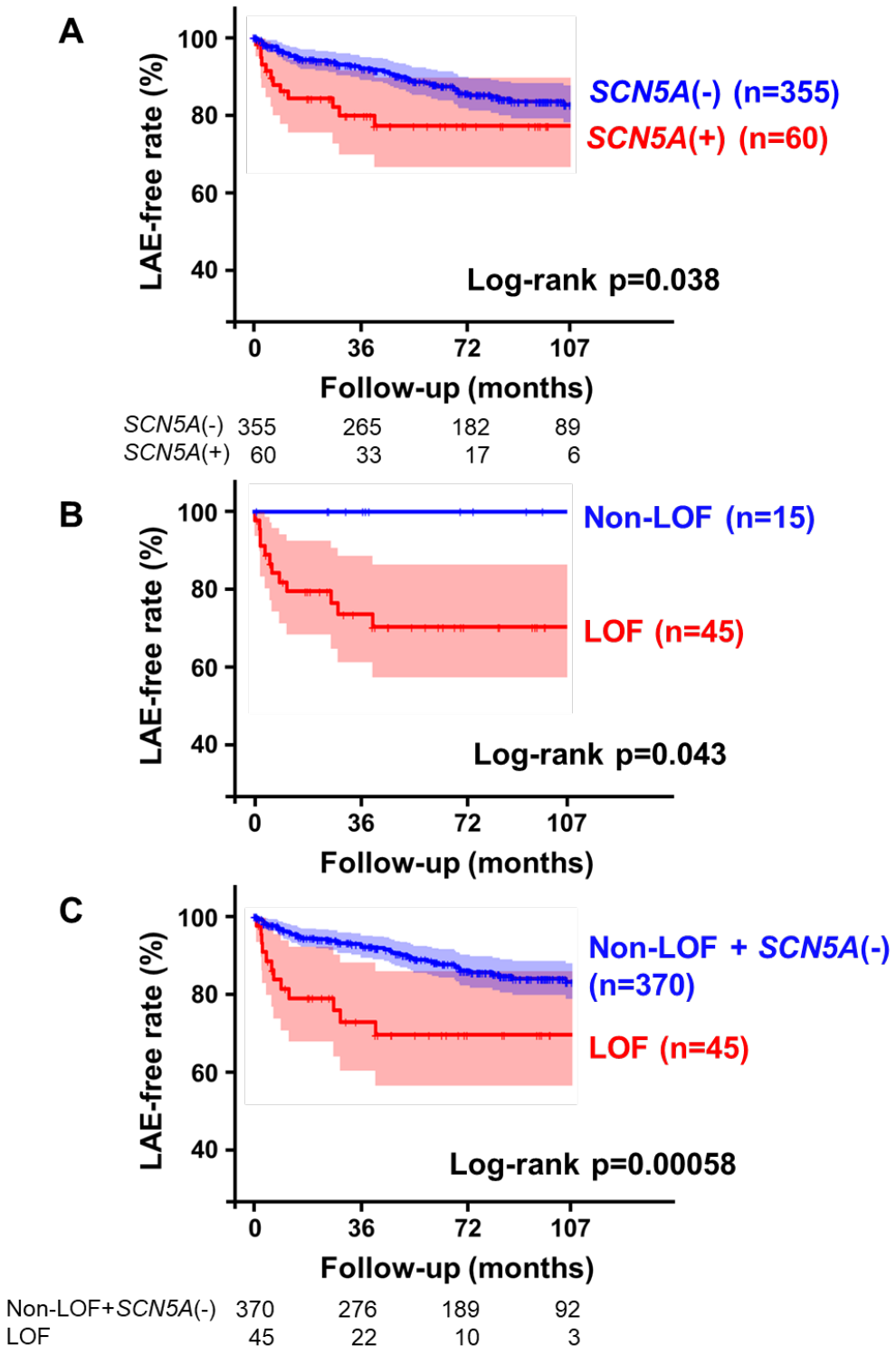

Figure S5. Stratified Kaplan–Meier analysis of lethal arrhythmic event-free survival during 107 months of follow-up in BrS cohort-I

To avoid the poor curve estimation in the Kaplan-Meier analysis due to small sample size and/or progressively enhanced suscetibility to lethal arrhythmic events (LAEs) in the loss-of-function (LOF)-*SCN5A* mutation carriers after 107 months (Figure 4), stratification analysis of LAE-survival during the first 107 months of follow-up was performend. **A**. LAE-free survival during the follow-up period in BrS probands carrying *SCN5A* rare variations (*SCN5A*(+); n=60) and *SCN5A*(-) (n=355). Confidence bands indicate 95% pointwise CI. **B**. Time course of BrS patients with LOF-*SCN5A* mutations (LOF, n=45), and Non-LOF (n=15). Non-LOF probands have no LAEs during the follow-up period. **C**. LAE-free survival of LOF (n=45) vs Non-LOF plus *SCN5A*(-) (n=370). These data are qualitatively similar to the Kaplan–Meier analysis of the entire mean follow-up period of 72 months (ranging from 1 to 249 months). (Figure 4)

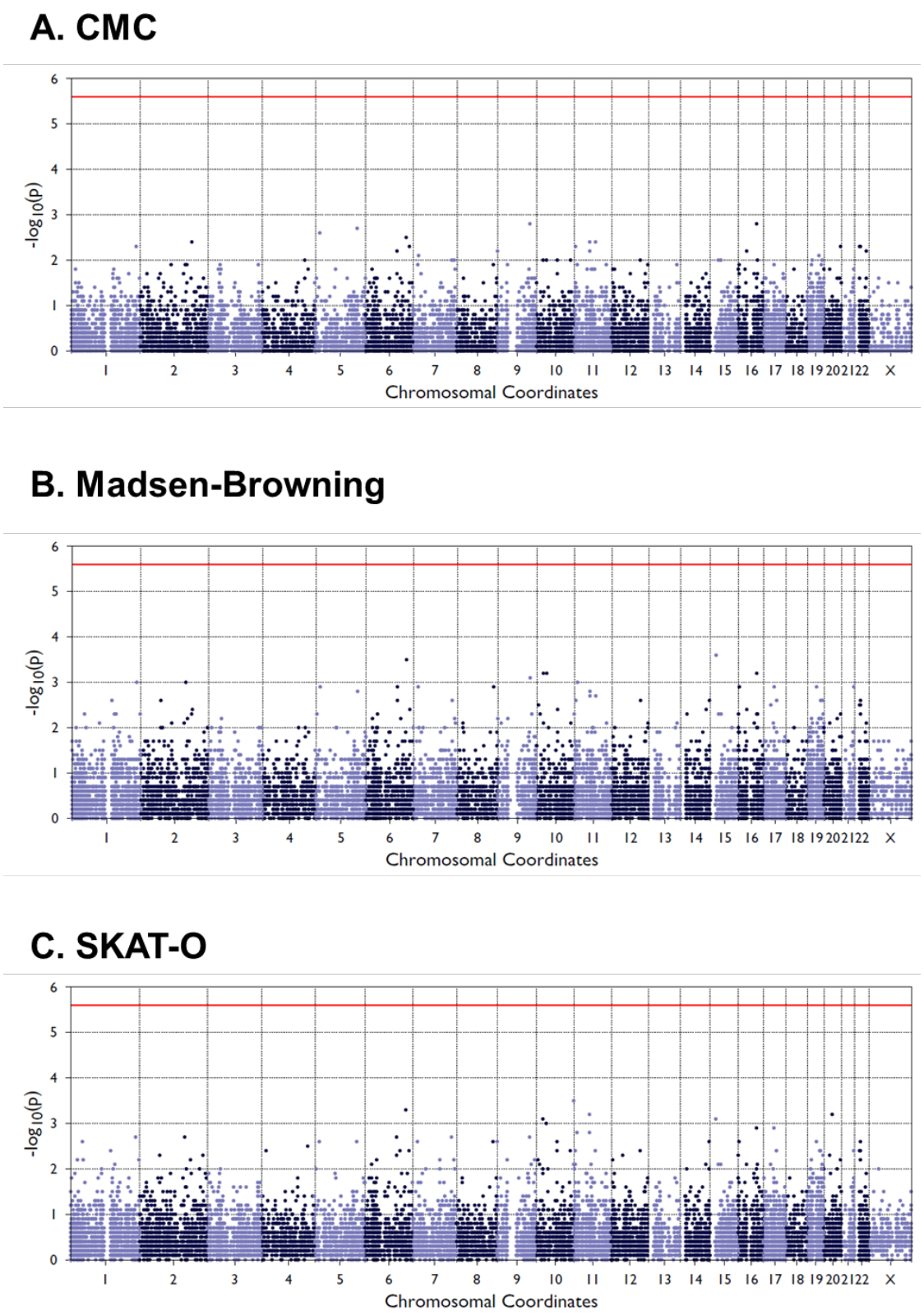

Figure S6. Manhattan plots for the gene-wise association tests
Results of gene-wise association of three different methods are shown; **A**. Burden test CMC, **B**. Madsen-Browning with adjusted weighs of variants and **C**. a combined test of burden and variance-component, SKAT-O. No genes exceeded the Bonferroni-adjusted gene-wise significance threshold ($p=2.94\times10^{-6}$; red lines) in three models.

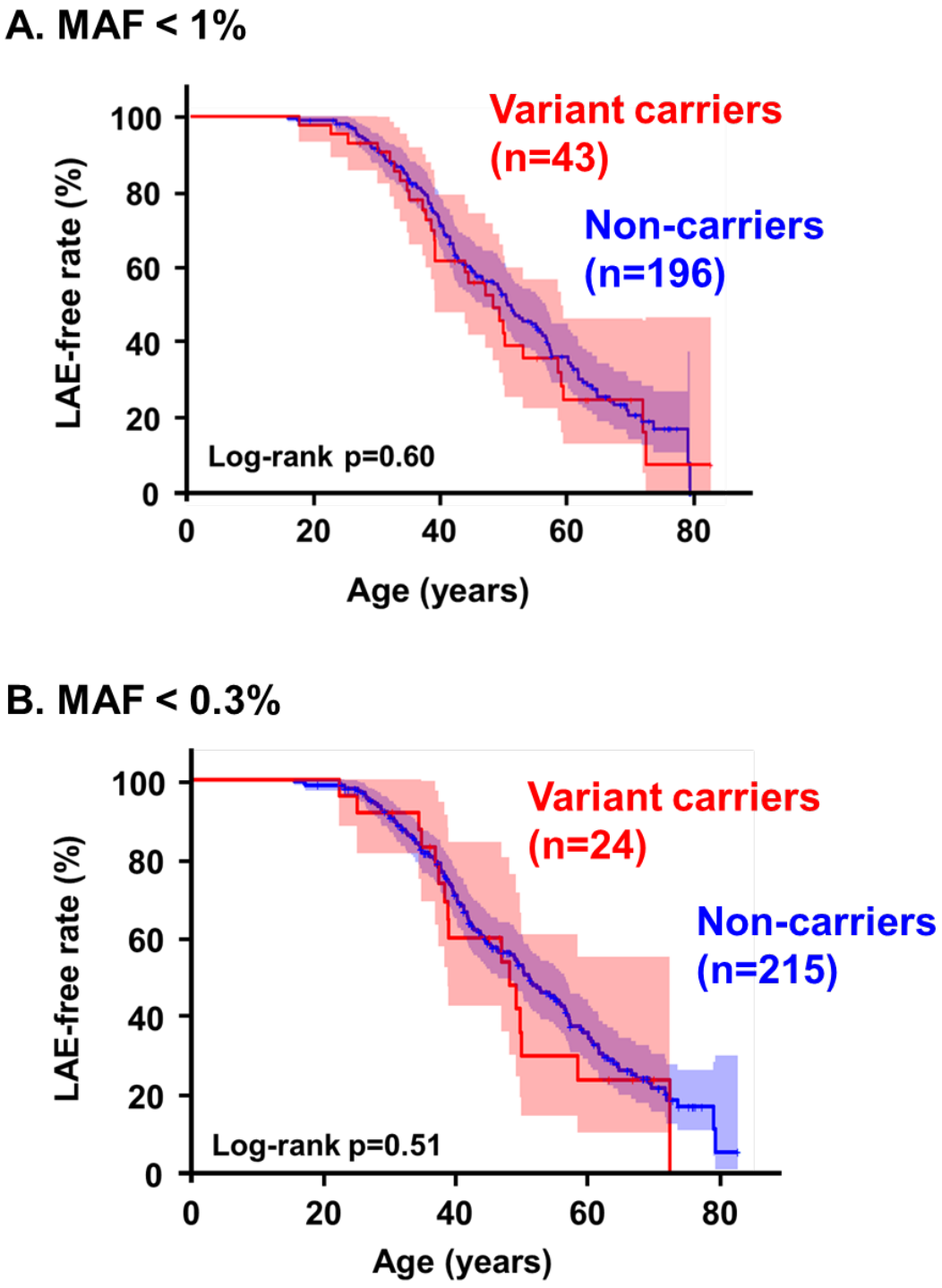

Figure S7. Prognostic effects of rare variations of *SCN5A*-modulating BrS-associated genes.
Kaplan-Meier analysis was performed to evaluate the LAE-free survival of BrS cohort-II probands with or without rare variants (**A**. MAF<1%; **B**: MAF<0.3%) of 8 *SCN5A*-modulating BrS-associated genes (*GPD1L, PKP2, MOG1, SCN10A, SCN1B, SCN2B, SCN3B*, and *SLMAP*). There were no significant differences in the prognosis of *SCN5A*(-) BrS probands regardless of the rare variations these genes in either cut-off MAF values. Probands without age information (n=49) were excluded from these analyses.

Table S1. Allele frequency and functional outcomes of 55 *SCN5A* variations in BrS cohort-I

(A) *SCN5A* variations functionally characterized elsewhere previously or null variations (n=33)

Protein	Position (GRCh37)	nucleotide	Type of mutations	Location	TM or non-TM	Minor allele frequency				Reference	%Peak INa density (of WT)
						gnomAD (global)	gnomAD (East Asian)	1000 Genomes	4.7KJPN (Japanese)		
R282H	3:38651314	c.G845A	missense	DI-S5/S6	TM	1.62E-05	5.80E-05	NR	NR	23	12%
R367H	3:38648200	c.G1100A		DI-S5/S6	TM	NR	NR			24	nonfunctional
R376H	3:38648173	c.G1127A		DI-S5/S6	TM	1.09E-05				25	30%
N406S	3:38647563	c.A1217G		DI-S6	TM	NR				8	gating abnormality
F532C	3:38645498	c.T1595G		IDL-I-II	non-TM	1.63E-05	2.33E-04		1.60E-03	26	100%
A735V	3:38639278	c.C2204T		DII-S1	TM	4.06E-06	5.80E-05		NR	27	23%
L846R	3:38627432	c.T2537G		DII-S5/S6	TM	NR	NR			28	nonfunctional
R878C	3:38627337	c.C2632T		DII-S5/S6	TM					29	nonfunctional
R893H	3:38627291	c.G2678A		DII-S5/S6	TM	4.06E-06	NR			2	nonfunctional
R1195H	3:38616870	c.G3584A		IDL-II-III	non-TM	NR				30	gating abnormality
V1328M	3:38601901	c.G3982A		DIII-S4/S5	TM					31	gating abnormality
G1408R	3:38601661	c.G4222A		DIII-S5/S6	TM					32	nonfunctional
A1428S	3:38598739	c.G4282T		DIII-S5/S6	TM	2.84E-05	4.06E-04	2.00E-04		33	62%
R1644C	3:38592933	c.C4930T		DIV-S4	TM	4.06E-06	NR	NR		34	gating abnormality
R1644H	3:38592932	c.G4931A		DIV-S4	TM	NR				35	late current
G1743R	3:38592636	c.G5227A		DIV-S5/S6	TM					36	nonfunctional
E1784K	3:38592513	c.G5350A		C-Terminal	non-TM					37	60%
del1380N	3:38601741	c.4140_4142delCAA	in-frame deletion	DIII-S5/S6	TM					38	nonfunctional
Q55X	3:38674636	c.C163T	nonsense	N-terminal	Not applicable	NR				39	null (PVS1), nonfunctional
R179X	3:38662410	c.C535T		DI-S2/S3	TM	4.07E-06				40	null (PVS1), nonfunctional
W904X	3:38627258	c.G2711A		DII-S5/S6	TM	NR				41	null (PVS1), nonfunctional
R1623X	3:38592996	c.C4867T		DIV-S4	TM					42	null (PVS1), nonfunctional
W1095X	3:38620931	c.G3285A		IDL-II-III	non-TM					**NA**	**null (PVS1)**
Y1409X	3:38601656	c.C4227G		DIII-S5/S6	TM						
N291TfsX52	3:38651289	c.870delC	frameshift	DI-S5/S6	TM						
R513VfsX8	3:38645556	c.1537delC		IDL-I-II	non-TM						
L1464WfsX5	3:38597973	c.4389_4396del CCTCTTTA		DIII-S6	TM						
L1579SfsX53	3:38595850	c.4732_4733dupAA		DIV-S2/S3	TM						
I1720SfsX67	3:38592706	c.5157delC		DIV-S5/S6	TM						
V1764SfsX23	3:38592573	c.5290delG		DIV-S6	TM						
IVS21+1G>A	3:38607899	c.3840+1G>A	splice site	DIII-S3	TM	8.13E-06					
IVS23+1G>A	3:38601636	c.4245+1G>A		DIII-S5/S6	TM	NR					
IVS24+1delG	3:38598721	c.4299+1delG		DIII-S5/S6	TM						

(B) *SCN5A* VUS (n=22)

Protein	Position (GRCh37)	nucleotide	Type of mutations	Location	TM or non-TM	Minor allele frequency				Reference
						gnomAD (global)	gnomAD (East Asian)	1000 Genomes	4.7KJPN (Japanese)	
R104Q	3:38671883	c.G311A	missense	N-terminal	non-TM	NR	NR	NR	NR	**NA**
L136P	3:38663966	c.T407C		DI-S1	TM					
L276Q	3:38651332	c.T827A		DI-S5	TM					
Y416C	3:38647533	c.A1247G		IDL-I-II	non-TM	4.06E-06				
E428K	3:38647498	c.G1282A		IDL-I-II	non-TM	5.42E-05	1.06E-04		3.00E-04	
R689H	3:38639416	c.G2066A		IDL-I-II	non-TM	1.02E-04	1.16E-04	2.00E-04	5.00E-04	
R693C	3:38639405	c.C2077T		IDL-I-II	non-TM	5.69E-05	5.80E-05	NR	NR	
Q779K	3:38628992	c.C2335A		DII-S2/S3	TM	NR	NR			
R814Q	3:38627528	c.G2441A		DII-S4	TM	2.55E-05	5.30E-05		1.00E-04	
R893C	3:38627292	c.C2677T		DII-S5/S6	TM	7.22E-06	NR		NR	
R988Q	3:38622687	c.G2963A		IDL-II-III	non-TM	4.87E-05	5.44E-05			
H1200Y	3:38616856	c.C3598T		IDL-II-III	non-TM	NR	NR		1.00E-04	
E1225K	3:38608067	c.G3673A		DIII-S1/S2	TM	4.06E-06		NR	NR	
T1247I	3:38608000	c.C3740T		DIII-S2	TM	3.25E-05				
V1405M	3:38601670	c.G4213A		DIII-S5/S6	TM	NR	NR		NR	
G1420R	3:38598763	c.G4258C		DIII-S5/S6	TM					
R1432S	3:38598725	c.G4296C		DIII-S5/S6	TM					
K1527R	3:38596003	c.A4580G		DIV-S1	TM					
T1709M	3:38592737	c.C5126T		DIV-S5/S6	TM	4.06E-06				
R1913C	3:38592126	c.C5737T		C-Terminal	non-TM	4.06E-06				
R1919H	3:38592107	c.G5756A		C-Terminal	non-TM	8.12E-06		2.00E-04		
H1923D	3:38592096	c.C5767G		C-Terminal	non-TM	NR		NR		

TM: Transmembrane region, D: Hydrophobic domain (DI-DIV) of Nav1.5, IDL: Interdomain linker region of Nav1.5, S: Transmembrane segment (S1-S6) of each domain of Nav1.5, NR: Not registered, NA: Not available, PVS1: null variants with very strong evidence of pathogenicity (ACMG-AMP)

Table S2. Electrophysiological properties of 22 *SCN5A* VUSs in BrS cohort-I

SCN5A VUS (n)	Peak INa density, pA/pF (%WT)	Activation		Steady-state inactivation		Recovery from inactivation					Functional category
		$V_{1/2}$ (mV)	*k* (mV)	$V_{1/2}$ (mV)	*k* (mV)	τ_{fast} (ms)	τ_{slow} (ms)	A_{fast}	A_{slow}	$t_{1/2}$ (ms)	
WT (14)	204.7 ± 89.2	-47.8 ± 3.7	-4.0 ± 0.8	-85.9 ± 5.4	6.3 ± 0.4	13.8 ± 7.4	100.5 ± 61.6	0.85 ± 0.05	0.13 ± 0.05	13.0 ± 7.1	**WT**
G1420R (12)	1.3 ± 2.3 (0.6%)‡	**Non-functional (n=4)**									**LOF (n=13)**
L276Q (8)	1.8 ± 0.9 (0.9%)‡										
R104Q (7)	2.1 ± 2.2 (1.0%)‡										
R893C (9)	6.6 ± 4.3 (3.2%)‡										
E1225K (18)	37.7 ± 23.3 (18.4%)‡	-35.0 ± 2.7†	-4.7 ± 0.4	-67.1 ± 4.2‡	5.5 ± 0.6*	3.4 ± 1.4‡	37.9 ± 33.2	0.76 ± 0.13	0.20 ± 0.13	3.3 ± 1.3†	
T1709M (9)	50.5 ± 29.2 (24.7%)‡	-50.0 ± 3.2	-4.4 ± 0.8	-89.7 ± 4.1	6.1 ± 1.0	13.9 ± 3.6	515.7 ± 446.5	0.86 ± 0.07	0.13 ± 0.07	11.5 ± 2.3	
V1405M (14)	55.5 ± 42.1 (27.1%)‡	-45.9 ± 5.7	-4.6 ± 1.0	-85.5 ± 6.3	6.3 ± 1.7	26.1 ± 17.7	106.4 ± 118.3	0.73 ± 0.12	0.24 ± 0.11	21.7 ± 12.3	
Y416C (12)	71.1 ± 35.9 (34.7%)‡	-48.0 ± 2.9	-6.2 ± 0.8‡	-97.1 ± 6.5‡	6.1 ± 0.7	46.6 ± 25.2†	136.8 ± 83.2	0.77 ± 0.07*	0.21 ± 0.07*	35.4 ± 16.1†	
R1913C (13)	79.8 ± 41.8 (39%)‡	-43.7 ± 3.0	-4.5 ± 0.7	-88.6 ± 4.8	6.6 ± 0.9	18.3 ± 11.7	218.8 ± 191.1	0.82 ± 0.05	0.16 ± 0.04	13.8 ± 6.8	
L136P (13)	96.7 ± 53.9 (47.2%)‡	-42.7 ± 3.7‡	-4.4 ± 0.7	-83.5 ± 4.5	6.1 ± 0.7	12.0 ± 4.1	141.6 ± 158.6	0.84 ± 0.06	0.13 ± 0.05	9.7 ± 2.7	
R1432S (12)	97 ± 47.6 (47.4%)‡	-45.9 ± 2.4	-4.5 ± 0.5	-88.1 ± 2.5	6.2 ± 0.6	22.5 ± 6.5	222.4 ± 181.2	0.86 ± 0.05	0.13 ± 0.05	14.4 ± 2.1	
R1919H (11)	103.2 ± 53.3 (50.4%)‡	-52.3 ± 4.0	-4.7 ± 0.7	-92.4 ± 6.0	6.8 ± 0.5	17.6 ± 11.1	159.7 ± 66.1	0.84 ± 0.04	0.15 ± 0.05	15.0 ± 9.0	
R693C (9)	108.9 ± 54.9 (53.2%)†	-54.9 ± 2.8†	-4.6 ± 0.5	-93.4 ± 5.0†	6.4 ± 0.6	22.8 ± 10.1	411.7 ± 603.3	0.87 ± 0.04	0.12 ± 0.03	18.8 ± 8.2	
R988Q (14)	134.3 ± 77.1 (65.6%)	-51.2 ± 3.9	-4.8 ± 0.4	-90.0 ± 5.6	7.2 ± 0.8	13.9 ± 5.5	145.9 ± 45.0	0.80 ± 0.06	0.19 ± 0.06	13.4 ± 5.6	**Non-LOF (n=9)**
R689H (9)	147.8 ± 64.2 (72.2%)	-49.2 ± 4.5	-3.8 ± 0.6	-86.9 ± 3.4	6.4 ± 0.7	12.8 ± 5.1	102.3 ± 52.3	0.85 ± 0.06	0.14 ± 0.06	11.7 ± 4.3	
E428K (8)	153.5 ± 99.8 (75%)	-51.6 ± 4.5	-3.7 ± 0.9	-87.7 ± 2.5	6.4 ± 0.7	11.8 ± 3.5	92.3 ± 57.7	0.84 ± 0.04	0.14 ± 0.04	10.0 ± 3.0	
Q779K (10)	157.7 ± 74.1 (77%)	-45.8 ± 4.1	-4.3 ± 1.0	-87.1 ± 6.0	6.2 ± 0.5	17.0 ± 9.0	108.1 ± 47.4	0.84 ± 0.05	0.14 ± 0.05	13.9 ± 6.3	
H1200Y (10)	166 ± 37.1 (81.1%)	-51.2 ± 4.3	-4.6 ± 0.4	-88.7 ± 4.6	6.7 ± 0.7	14.0 ± 3.7	121.1 ± 54.0	0.82 ± 0.04	0.16 ± 0.04	12.5 ± 3.7	
K1527R (7)	174.6 ± 65.0 (85.3%)	-52.0 ± 3.3	-3.6 ± 0.5	-87.2 ± 3.8	6.6 ± 0.3	14.8 ± 6.0	107.8 ± 27.4	0.86 ± 0.11	0.12 ± 0.11	12.8 ± 7.8	
T1247I (12)	179.5 ± 48.3 (87.7%)	-52.2 ± 2.1	-4.4 ± 0.7	-87.3 ± 3.0	7.7 ± 0.6‡	17.1 ± 4.8	180.6 ± 57.2	0.81 ± 0.03	0.18 ± 0.03	15.6 ± 4.3	
H1923D (12)	189.1 ± 62.7 (92.4%)	-50.5 ± 4.5	-3.7 ± 0.5	-86.4 ± 4.7	6.5 ± 0.7	16.0 ± 9.1	154.7 ± 169.6	0.85 ± 0.05	0.14 ± 0.05	12.6 ± 6.2	
R814Q (12)	222.5 ± 89.3 (108.7%)	-52.7 ± 3.0	-4.9 ± 0.5*	-88.2 ± 3.9	7.5 ± 0.8†	18.3 ± 5.4	273.3 ± 122.5	0.85 ± 0.02	0.14 ± 0.02	17.1 ± 4.2	

LOF and Non-LOF: Variants with or without significantly reduced peak current densities than WT, respectively. The border zone of LOF/ Non-LOF was between 53.2% (R693C) and 65.6% (R988Q). Statistical analysis was performed using one-way ANOVA followed by Bonferroni's post-hoc comparison test. * <0.05; † <0.01; ‡ <0.001, LOF: loss-of-function

Table S3. Experimental conditions of the current and previous patch clamp studies

Mutation	Functional classification	Cell	alpha subunit (GenBank)	beta subunit co-expression	Time after transfection	First author	Year	Reference
Current study		HEK293T	NM_000335	no	24-48 hr			
Q55X	LOF	HEK293T	NM_000335	no	ND	Makita	2007	39*
R179X		HEK293	NM_000335	beta1	24-48 hr	Kawamura	2009	40
W904X		ND	NM_000335	ND	ND	Makiyama	2010	41
R1623X		HEK293	NM_000335	beta1	24-72 hr	Benson	2003	42
R367H		HEK293T	NM_000335	no	ND	Takehara	2004	24*
L846R		HEK293T	NM_000335	beta1	24-72 hr	Watanabe	2011	28*
R878C		HEK293	M77235	no/beta1	24 hr	Zhang	2008	29
R893H		ND	ND	ND	ND	Kapplinger	2015	2
del1380N		HEK293	ND	no	ND	Yang	2017	38
G1408R		COS-7	ND	no/beta1	ND	Kyndt	2001	32
G1743R		HEK293	NM_000335	no	24-48hr	Valdivia	2004	36
R282H		HEK293	NM_000335	beta1	ND	Itoh	2005	23
R376H		HEK293	ND	beta1	48hr	Rossenbacker	2004	25
A735V		HEK293	ND	no	ND	de la Roche	2019	27
A1428S		HEK293	ND	no	ND	Zhu	2015	33
E1784K		HEK293T	NM_000335	beta1	24–72 hr	Makita	2008	37*
N406S	Non-LOF	HEK293	NM_000335	beta1	ND	Itoh	2005	8
R1195H		HEK293	NM_000335	no	24 hr	Medeiros-Domingo	2009	30
V1328M		HEK293	NM_000335	no	48-72 hr	Turker	2016	31
R1644C		HEK293	ND	beta1	ND	Frustaci	2005	34
R1644H		HEK293T	ND	no	ND	Wang	1996	35
F532C		HEK293T	NM_000335	beta1	24-72 hr	Otagiri	2008	26*

HEK293: Human Embryonic Kidney 293 cell, ND: Not described, *: Our previous studies

Table S4. Genetic, functional, clinical characteristics, and *in silico* prediction data of 55 *SCN5A* rare variations in BrS cohort-I

Functional subgroups	Genomic position (GRCh37)	nucleotide	protein	dbSNP	Type of mutation	Location	Functional consequences (% I_{Na} density vs WT, gating)	Reference	Probands (n)	History of ACA	LAE during F/U	Overall LAE	Minor allele frequency				*In silico* predictions						
													gnomAD (global)	gnomAD (East Asian)	1000 Genomes	4.7K JPN	SIFT	PolyPhen-2	Species	Paralogue	Grantham	Condel	Mutation Assessor
LOF (n=40)	3:38674636	c.C163T	p.Q55X		nonsense	N-terminal	nonfunctional	39	1				NR	NR	NR	NR	NA	NA	-	-	-	-	-
	3:38671883	c.G311A	p.R104Q	rs199473554	missense	N-terminal	nonfunctional	This study	1				NR	NR	NR	NR	0(D)	1.000(PD)	1	1	43	0.684 (D)	3.52 (H)
	3:38663966	c.T407C	p.L136P	rs199473557	missense	DI-S1	49%, gating abnormality	This study	2*				NR	NR	NR	NR	0(D)	0.739(PoD)	0	0	98	0.576 (D)	2.135 (M)
	3:38662410	c.C535T	p.R179X		nonsense	DI-S2/S3	nonfunctional	40	1	yes	yes	yes	4.07E-06	NR	NR	NR	NA	NA	-	-	-	-	-
	3:38651332	c.T827A	p.L276Q	rs199473081	missense	DI-S5	nonfunctional	This study	1	yes		yes	NR	NR	NR	NR	0(D)	1.000(PD)	1	1	113	0.695 (D)	3.61 (H)
	3:38651314	c.G845A	p.R282H	rs199473083	missense	DI-S5/S6	12%	23	3*	yes		yes	1.62E-05	5.80E-05	NR	NR	0.04(D)	1.000(PD)	0	0	29	0.588 (D)	1.535 (L)
	3:38651289	c.870delC	p.N291TfsX52		frame shift	DI-S5/S6	null (PVS1)		1	yes		yes	NR	NR	NR	NR	NA	NA	-	-	-	-	-
	3:38648200	c.G1100A	p.R367H	rs28937318	missense	DI-S5/S6	nonfunctional	24	1		yes	yes	NR	NR	NR	NR	0(D)	1.000(PD)	1	1	29	0.692 (D)	3.43 (M)
	3:38648173	c.G1127A	p.R376H	rs199473101	missense	DI-S5/S6	30%	25	1	yes	yes	yes	1.09E-05	NR	NR	NR	0(D)	1.000(PD)	0	0	29	0.572 (D)	2.78 (M)
	3:38647533	c.A1247G	p.Y416C	rs372395294	missense	IDL-I-II	36%, gating abnormality	This study	1				4.06E-06	NR	NR	NR	0(D)	1.000(PD)	1	1	194	0.65 (D)	3.005 (M)
	3:38645556	c.1537delC	p.R513VfsX8		frame shift	IDL-I-II	null (PVS1)		1				NR	NR	2.00E-04	NR	NA	NA	-	-	-	-	-
	3:38639405	c.C2077T	p.R693C	rs375306544	missense	IDL-I-II	55%, gating abnormality	This study	1	yes	yes	yes	5.69E-05	5.80E-05	NR	NR	0.1(T)	0.660(PoD)	0	0	180	0.547 (D)	1.95 (M)
	3:38639278	c.C2204T	p.A735V	rs137854611	missense	DII-S1	23%, gating abnormality	27	1	yes	yes	yes	4.06E-06	5.80E-05	NR	NR	0(D)	0.049(B)	1	1	64	0.692 (D)	3.83 (H)
	3:38627432	c.T2537G	p.L846R		missense	DII-S5/S6	nonfunctional	28	1	yes		yes	NR	NR	NR	NR	0(D)	0.999(PD)	1	1	102	0.762 (D)	4.56 (H)
	3:38627337	c.C2632T	p.R878C		missense	DII-S5/S6	nonfunctional	29	1				NR	NR	NR	NR	0(D)	1.000(PD)	1	0	180	0.747 (D)	4.48 (H)
	3:38627292	c.C2677T	p.R893C	rs199473171	missense	DII-S5/S6	nonfunctional	This study	1		yes	yes	7.22E-06	NR	NR	NR	0(D)	1.000(PD)	1	1	180	0.756 (D)	4.455 (H)
	3:38627291	c.G2678A	p.R893H	rs199473172	missense	DII-S5/S6	nonfunctional	2	1				4.06E-06	NR	NR	NR	0(D)	1.000(PD)	1	1	29	0.731 (D)	4.455 (H)
	3:38627258	c.G2711A	p.W904X		nonsense	DII-S5/S6	nonfunctional	41	1				NR	NR	NR	NR	NA	NA	-	-	-	-	-
	3:38620931	c.G3285A	p.W1095X		nonsense	IDL-II-III	null (PVS1)		1				NR	NR	NR	NR	NA	NA	-	-	-	-	-
	3:38608067	c.G3673A	p.E1225K	rs199473204	missense	DIII-S1/S2	19%, gating abnormality	This study	2*				4.06E-06	NR	NR	NR	0(D)	1.000(PD)	0	1	56	0.706 (D)	3.805 (H)
	3:38601741	c.4140_4142 delCAA	p.del1380N		deletion	DIII-S5/S6	nonfunctional	38	1				NR	NR	NR	NR	NA	NA	-	-	-	-	-
	3:38601670	c.G4213A	p.V1405M	rs199473239	missense	DIII-S5/S6	28%, gating abnormality	This study	1				NR	NR	NR	NR	0(D)	1.000(PD)	1	1	21	0.694 (D)	3.8 (H)
	3:38601661	c.G4222A	p.G1408R	rs137854612	missense	DIII-S5/S6	nonfunctional	32	1				NR	NR	NR	NR	0(D)	1.000(PD)	1	0	125	0.711 (D)	4.655 (H)
	3:38601656	c.C4227G	p.Y1409X		nonsense	DIII-S5/S6	null (PVS1)		1				NR	NR	NR	NR	NA	NA	-	-	-	-	-
	3:38598763	c.G4258C	p.G1420R	rs199473611	missense	DIII-S5/S6	nonfunctional	This study	1				NR	NR	NR	NR	0(D)	1.000(PD)	1	1	125	0.803 (D)	5.01 (H)
	3:38598739	c.G4282T	p.A1428S	rs200034939	missense	DIII-S5/S6	62%	33	1	yes	yes	yes	2.84E-05	4.06E-04	2.00E-04	NR	0(D)	1.000(PD)	1	1	99	0.593 (D)	2.44 (M)
	3:38598725	c.G4296C	p.R1432S		missense	DIII-S5/S6	49%	This study	1				NR	NR	NR	NR	0(D)	0.947(PoD)	1	0	110	0.605 (D)	2.755 (M)
	3:38597973	c.4389_4396del CCTCTTTA	p.L1464WfsX5		frame shift	DIII-S6	null (PVS1)		1				NR	NR	NR	NR	NA	NA	-	-	-	-	-
	3:38595850	c.4732_4733 dupAA	p.L1579SfsX53		frame shift	DIV-S2/S3	null (PVS1)		1				NR	NR	NR	NR	NA	NA	-	-	-	-	-
	3:38592996	c.C4867T	p.R1623X		nonsense	DIV-S4	null (PVS1)	42	1	yes		yes	NR	NR	NR	NR	NA	NA	-	-	-	-	-
	3:38592737	c.C5126T	p.T1709M	rs199473297	missense	DIV-S5/S6	28%	This study	1		yes	yes	4.06E-06	NR	NR	NR	0(D)	1.000(PD)	1	1	81	0.751 (D)	5.14 (H)
	3:38592706	c.5157delC	p.I1720SfsX67		frame shift	DIV-S5/S6	null (PVS1)		1		yes	yes	NR	NR	NR	NR	NA	NA	-	-	-	-	-
	3:38592636	c.G5227A	p.G1743R	rs199473629	missense	DIV-S5/S6	nonfunctional	36	1	yes		yes	NR	NR	NR	NR	0(D)	1.000(PD)	1	0	125	0.758 (D)	3.585 (H)
	3:38592513	c.G5350A	p.E1784K	rs137854601	missense	C-Terminal	60%, gating abnormality	37	2*	yes	yes	yes	NR	NR	NR	NR	0(D)	0.820(PoD)	1	0	56	0.595 (D)	2.125 (M)
	3:38592126	c.C5737T	p.R1913C	rs755182182	missense	C-Terminal	40%, gating abnormality	This study	1				4.06E-06	NR	NR	NR	0(D)	1.000(PD)	1	1	180	0.68 (D)	3.81 (H)
	3:38592107	c.G5756A	p.R1919H	rs141107387	missense	C-Terminal	52%, gating abnormality	This study	1				8.12E-06	NR	2.00E-04	NR	0.05(D)	0.914(PoD)	1	0	29	0.603 (D)	2.985 (M)
	3:38592573	c.5290delG	p.V1764SfsX23		frame shift	DIV-S6	null (PVS1)		1				NR	NR	NR	NR	NA	NA	-	-	-	-	-
	3:38607899	IVS21+1G>A	-		splice donor	DIII-S3	null (PVS1)		1	yes	yes	yes	8.13E-06	NR	NR	NR	NA	NA	-	-	-	-	-
	3:38601636	IVS23+1G>A	-		splice donor	DIII-S5/S6	null (PVS1)		1				NR	NR	NR	NR	NA	NA	-	-	-	-	-
	3:38598721	IVS24+1delG	-		splice donor	DIII-S5/S6	null (PVS1)		1				NR	NR	NR	NR	NA	NA	-	-	-	-	-
Non-LOF (n=15)	3:38647563	c.A1217G	p.N406S	rs199473568	missense	DI-S6	gating abnormality	8	1				NR	NR	NR	NR	0(D)	0.999(PD)	1	1	46	0.674 (D)	2.875 (M)
	3:38647498	c.G1282A	p.E428K	rs199473111	missense	IDL-I-II	normal	This study	1				5.42E-05	1.06E-04	NR	3.00E-04	0.07(T)	0.041(B)	0	0	56	0.557 (D)	1.04 (L)
	3:38645498	c.T1595G	p.F532C	rs199473573	missense	IDL-I-II	normal	26	1				1.63E-05	2.33E-04	NR	1.60E-03	0.01(D)	0.999(PD)	1	0	205	0.636 (D)	2.935 (M)
	3:38639416	c.G2066A	p.R689H	rs199473145	missense	IDL-I-II	normal	This study	1				1.02E-04	1.16E-04	2.00E-04	5.00E-04	0.04(D)	0.004(B)	0	0	29	0.553 (D)	0.71 (N)
	3:38628992	c.C2335A	p.Q779K	rs199473583	missense	DII-S2/S3	normal	This study	1				NR	NR	NR	NR	0.18(T)	0.005(B)	0	0	53	0.558 (D)	0.59 (N)
	3:38627528	c.G2441A	p.R814Q	rs199473584	missense	DII-S4	normal	This study	1	yes		yes	2.55E-05	5.30E-05	NR	1.00E-04	0(D)	0.999(PD)	1	1	43	0.742 (D)	4.755 (H)
	3:38622687	c.G2963A	p.R988Q	rs759584454	missense	IDL-II-III	normal	This study	1				4.87E-05	5.44E-05	NR	NR	0.01(D)	0.001(B)	0	0	43	0.533 (D)	1.055 (L)
	3:38616870	c.G3584A	p.R1195H	rs199473596	missense	IDL-II-III	gating abnormality	30	1				NR	NR	NR	NR	0(D)	1.000(PD)	1	1	29	0.667 (D)	3.61 (H)
	3:38616856	c.C3598T	p.H1200Y	rs1416591678	missense	IDL-II-III	normal	This study	1				NR	NR	NR	1.00E-04	0.01(D)	0.002(B)	0	0	83	0.523 (D)	0.695 (N)
	3:38608000	c.C3740T	p.T1247I	rs764018276	missense	DIII-S2	normal	This study	1	yes		yes	3.25E-05	NR	NR	NR	0(D)	0.938(PoD)	0	1	89	0.667 (D)	3.295 (M)
	3:38601901	c.G3982A	p.V1328M		missense	DIII-S4/S5	gating abnormality	31	1				NR	NR	NR	NR	0(D)	0.988(PD)	0	0	21	0.585 (D)	1.51 (L)
	3:38596003	c.A4580G	p.K1527R	rs199473270	missense	DIV-S1	normal	This study	1				NR	NR	NR	NR	0.87(T)	0.077(B)	0	0	26	0.61 (D)	2.15 (M)
	3:38592933	c.C4930T	p.R1644C	rs199473287	missense	DIV-S4	gating abnormality	34	1				4.06E-06	NR	NR	NR	0(D)	1.000(PD)	1	1	180	0.782 (D)	4.975 (H)
	3:38592932	c.G4931A	p.R1644H		missense	DIV-S4	late current	35	1				NR	NR	NR	NR	0(D)	0.995(PD)	1	1	29	0.705 (D)	3.69 (H)
	3:38592096	c.C5767G	p.H1923D		missense	C-Terminal	normal	This study	1				NR	NR	NR	NR	0.13(T)	0.209(B)	0	0	81	0.552 (D)	1.795 (L)

ACA: aborted cardiac arrest, ICD: implantable cardioverter defibrillator, F/U: follow-up, gnomAD: The Genome Aggregation Database, 4.7KJPN: ToMMo-4.7KJPN database, SIFT: Sorting Intolerant From Tolerant, PolyPhen-2: Polymorphism Phenotyping v2, CADD: Combined Annotation-Dependent Depletion, M-CAP: Mendelian Clinically Applicable Pathogenicity, VUS: variants of unknown significance, NA: not applicable, NR: Not registered, PD: probably damaging, PoD: possibly damaging, P:Pathogenic, B: benign, D: deleterious, T: tolerated, DC: disease causing, H: high, M: middle, L: low, N: neutral, Asterisks: mutations identified in multiple probands, but there were no close familial relationship among them.

Table S5. ECG parameters of patients of different subgroups in BrS-cohort-I

Patient subgroups (n)		P wave duration (ms)	PQ interval (ms)	QRS duration (ms)			S duration (ms)	
		II	II	II	V2	V5	II	V5
LOF (45)		122.5 ± 25.8	221.4 ± 48.0	105.0 ± 27.0	112.8 ± 21.5	106.8 ± 24	38.4 ± 26.4	48.0 ± 24.4
Non-LOF (15)		101.5 ± 24.7	192.7 ± 30.6	92.1 ± 13.7	97.9 ± 16.9	90.5 ± 18.9	45.5 ± 28.1	40.4 ± 15.7
***SCN5A*(-)** (355)		93.3 ± 14.8	175.8 ± 25.2	86.1 ± 16.7	93.7 ± 14.8	87.1 ± 16.8	31 ± 20.9	33.6 ± 19.4
P values	**LOF vs Non-LOF vs *SCN5A*(-)**	<0.0001	<0.0001	<0.0001	<0.0001	<0.0001	0.02	<0.0001
	LOF vs Non-LOF	0.011	0.11	0.65	0.047	0.02	1	0.71
	LOF vs *SCN5A*(-)	<0.0001	<0.0001	<0.0001	<0.0001	<0.0001	0.16	<0.0001

Patient subgroups (n)		S amplitude (mV)		RR interval (ms)	QTc (ms)		
		II	V5	II	II	V2	V5
LOF (45)		0.3 ± 0.4	0.7 ± 1.0	921.5 ± 196.4	390.9 ± 35.6	405.2 ± 45.9	392.1 ± 34.5
Non-LOF (15)		0.3 ± 0.2	0.5 ± 0.4	867.7 ± 179.9	404.2 ± 33.9	410.4 ± 46.4	399.3 ± 32.1
***SCN5A*(-)** (355)		0.5 ± 0.9	0.7 ± 1.3	896.7 ± 153.9	385.6 ± 28.8	389.3 ± 35.6	383.5 ± 29.7
P values	**LOF vs Non-LOF vs *SCN5A*(-)**	0.76	0.01	0.90	0.12	0.01	0.06
	LOF vs Non-LOF	NA	1	NA	NA	1	NA
	LOF vs *SCN5A*(-)	NA	0.01	NA	NA	0.047	NA

Statistical analysis was performed using Kruskal-Wallis test followed by Dunn's test. *SCN5A*(-): *SCN5A* mutation non-carriers, NA: Not Applicable.

Table S6. Sensitivity analyses using bootstrap method

A. LAEs in BrS-I subgroups classified by different *SCN5A* functional properties

Subgroups	Annual event rate [%/year (95% CI)]
All BrS	2.48 (1.85-3.12)
SCN5A (-)	2.17 (1.62-2.83)
SCN5A (+)	5.19 (2.37-8.49)
LOF	8.29 (3.99-14.61)
Non-LOF	0
Non-LOF+*SCN5A* (-)	2.10 (1.46-2.74)

B. Univariate analysis

Variables	HR (95% CI)
History of aborted cardiac arrest	6.77 (4.16-11.42)
LOF-*SCN5A* mutations	3.10 (1.57-5.76)
In silico -predicted rare *SCN5A* variants	2.09 (1.11-3.72)
History of syncope	2.04 (0.86-4.5)
Male	NA
VT/VF by programmed electrical stimulation	1.76 (1.04-2.97)
Family history of sudden cardiac death	1.09 (0.50-1.98)
Documented atrial fibrillation	1.82 (0.95-3.15)
Late potential positive	1.54 (0.80-3.58)
Spontaneous type-I ST elevation	1.38 (0.81-2.76)
QRS (V5)≥120 ms	2.53 (1.22-4.88)
P (II)≥120 ms	2.67 (1.41-4.63)

C. Multivariate analysis

Variables	LOF-*SCN5A* mutations [HR (95% CI)]	*In silico* -predicted rare *SCN5A* variants [HR (95% CI)]
History of aborted cardiac arrest	6.65 (3.5-11.94)	6.75 (3.88-12.41)
SCN5A status	2.98 (1.31-6.08)	2.06 (1.004-4.16)
QRS (V5)≥120 ms	1.13 (0.44-2.63)	1.25 (0.43-2.96)
Documented atrial fibrillation	0.99 (0.47-1.83)	0.96 (0.47-1.82)

NA: data not available

Table S7. Rare variations (MAF<1%) of non-*SCN5A* BrS-associated genes identified by whole-exome sequencing in BrS cohort-II (n=288) and controls (n=372)

Chromosome	Position (GRCh37)	Reference allele	Alternative allele	Gene*	call rate	Cases (n)	Controls (n)	Type of variant	Amino acid	dbSNP	ClinVar	Minor allele frequency			
												gnomAD-global	gnomAD East Asian	1000Genomes	4.7KJPN
12	2,229,579	G	A	*CACNA1C*	99.7%	0	1	missense	A154T			1.2.E-05	none	none	none
	2,566,783	C	T		99.7%	1	0	missense	A223V			none	none	none	none
	2,676,738	C	T		99.7%	0	4	missense	T558M	rs572234918	Uncertain significance	1.2.E-04	9.3.E-04	6.0.E-04	6.0.E-04
	2,760,761	C	G		100.0%	2	2	missense	P1323A	rs201551454	Uncertain significance	5.7.E-05	3.6.E-04	2.0.E-04	2.8.E-03
	2,788,865	G	T		100.0%	1	1	missense	G1783C	rs781633980		1.2.E-05	none	none	1.6.E-03
	2,789,572	G	A		97.8%	1	1	missense	A1830T			2.5.E-04	none	none	none
	2,791,780	T	A		96.6%	0	1	missense	Y1908N			none	none	none	none
	2,797,760	G	A		99.9%	0	1	missense	E2061K			1.2.E-05	none	none	none
7	81,746,437	A	G	*CACNA2D1*	99.6%	0	1	missense	I150T			4.0.E-06	none	none	none
3	32,200,533	G	A	*GPD1L*	99.9%	2	0	missense	D262N	rs746057191		1.4.E-05	none	none	1.0.E-04
15	73,615,370	G	A	*HCN4*	99.3%	0	1	nonsense	R1022X			2.7.E-05	none	none	none
	73,615,517	C	T		99.3%	2	0	missense	G973R			9.2.E-05	none	none	none
	73,615,589	G	A		99.3%	2	2	missense	R949W	rs755614529		1.3.E-04	9.8.E-04	none	1.8.E-03
	73,616,270	G	A		99.7%	1	0	missense	L722F	rs774364558		8.3.E-06	1.1.E-04	none	2.0.E-04
	73,617,719	C	T		98.2%	1	0	missense	D553N	rs104894485	Pathogenic	3.6.E-05	none	2.0.E-04	8.0.E-04
	73,622,030	C	T		100.0%	1	0	missense	V492I	rs772144022		1.6.E-05	5.4.E-05	none	2.0.E-04
	73,622,056	C	T		99.6%	0	1	missense	R483Q	rs998387579	Uncertain significance	3.2.E-05	4.5.E-04	none	1.0.E-04
	73,660,028	G	A		97.2%	1	1	missense	A195V	rs201375192	Uncertain significance	3.7.E-04	4.9.E-03	8.0.E-04	9.0.E-04
1	112,525,026	T	C	*KCND3*	100.0%	1	0	missense	Y108C			4.0.E-06	5.4.E-05	none	1.0.E-04
11	74,168,313	C	T	*KCNE3*	100.0%	0	1	missense	R99H	rs121908441	Conflicting interpretations of pathogenicity	9.2.E-05	2.0.E-04	6.0.E-04	9.0.E-04
	74,168,599	T	C		98.5%	0	1	missense	T4A	rs200856070	Conflicting interpretations of pathogenicity	1.3.E-04	1.8.E-03	6.0.E-04	9.0.E-04
7	150,647,198	G	A	*KCNH2*	100.0%	1	0	missense	A819V	rs774109163		4.0.E-06	none	none	none
	150,656,677	G	A		98.7%	1	0	missense	T152I			4.0.E-06	none	none	none
	150,656,690	G	A		98.7%	0	1	missense	R148W	rs139544114	Conflicting interpretations of pathogenicity	1.1.E-03	none	none	2.0.E-04
	150,656,717	C	T		100.0%	0	1	missense	G139R			8.0.E-06	none	none	none
12	21,919,112	G	A	*KCNJ8*	100.0%	0	1	missense	R274C			3.2.E-05	none	none	5.0.E-04
	21,926,454	T	C		100.0%	0	1	missense	K33E			none	none	none	5.0.E-04
12	32,949,098	C	T	*PKP2*	96.4%	3	4	missense	D812N	rs200947767	Uncertain significance	5.3.E-05	2.0.E-04	4.0.E-04	2.7.E-03
	32,949,229	T	G		98.4%	1	3	missense	K768T	rs201487421	Uncertain significance	5.6.E-05	7.7.E-04	6.0.E-04	3.7.E-03
	33,030,829	T	C		99.9%	2	0	missense	S329G	rs779173447		1.1.E-05	none	none	3.0.E-04
	33,031,089	G	A		100.0%	2	2	missense	T242M	rs201580443	Uncertain significance	1.2.E-04	1.2.E-03	2.0.E-04	1.3.E-03
17	8,192,348	T	C	*MOG1*	99.7%	0	1	missense	L51P			none	none	none	none
	8,192,767	G	A		100.0%	0	3	missense	G129D			none	none	none	none
3	38,739,034	C	T	*SCN10A*	100.0%	0	1	missense	G1893S			none	none	none	none
	38,739,106	G	A		100.0%	0	4	missense	R1869C	rs141648641	Likely benign	9.1.E-04	1.5.E-03	2.0.E-04	1.9.E-03
	38,739,123	C	T		100.0%	2	0	missense	R1863Q	rs191869263		2.4.E-05	2.7.E-04	2.0.E-04	5.0.E-04
	38,739,175	G	T		100.0%	1	1	missense	L1846I	rs1001583386		none	none	none	2.3.E-03
	38,739,595	T	C		100.0%	0	3	missense	I1706V			none	none	none	none
	38,739,664	G	A		100.0%	5	2	missense	P1683S	rs146999807	Benign	9.0.E-04	8.4.E-03	2.4.E-03	6.1.E-03
	38,739,687	G	A		100.0%	0	1	missense	P1675L	rs564943632		4.0.E-06	none	6.0.E-04	3.0.E-04
	38,740,013	G	C		98.1%	0	1	nonsense	Y1566X			none	none	none	none
	38,740,041	G	GA		98.1%	1	0	frameshift	S1559FfsX4			4.0.E-06	none	none	1.0.E-04
	38,752,339	C	T		97.3%	2	0	missense	R1380Q	rs149155352	Uncertain significance	7.1.E-05	none	2.0.E-04	1.4.E-03
	38,753,757	G	T		99.9%	1	0	missense	N1328K	rs1204063286		none	none	none	4.0.E-04
	38,753,897	T	C		99.1%	0	1	missense	M1282V	rs1006794198		none	none	none	5.0.E-04
	38,760,283	G	A		99.7%	4	5	missense	T1181M	rs150773437	Benign	7.2.E-04	9.3.E-03	2.2.E-03	3.2.E-03

Table S7 (continue)

Chromosome	Position (GRCh37)	Reference allele	Alternative allele	Gene *	call rate	Cases (n)	Controls (n)	Type of variant	Amino acid	dbSNP	ClinVar	Minor allele frequency			
												gnomAD-global	gnomAD East Asian	1000Genomes	4.7KJPN
3	38,760,318	C	T	*SCN10A*	98.1%	0	1	splicing	c.3508-1C>T			none	none	none	none
	38,770,142	C	T		99.3%	0	1	missense	R844H	rs562091549		2.4.E-05	none	2.0.E-04	5.0.E-04
	38,770,188	G	A		100.0%	1	0	missense	R829C	rs755974168		4.0.E-06	none	none	1.0.E-04
	38,770,244	C	T		100.0%	0	1	missense	G810E			none	none	none	none
	38,770,349	G	A		100.0%	1	0	missense	T775I	rs150501065		1.7.E-04	2.3.E-03	4.0.E-04	4.0.E-04
	38,783,842	C	T		97.3%	0	1	missense	M682I			none	none	none	none
	38,793,756	T	G		98.1%	0	1	missense	Q570P			none	none	none	2.0.E-04
	38,793,972	C	T		99.0%	1	0	missense	R498Q			1.9.E-04	2.6.E-04	4.0.E-04	none
	38,798,298	A	C		99.3%	6	4	missense	F386C	rs78555408	Benign	4.9.E-04	6.7.E-03	1.8.E-03	3.7.E-03
	38,798,514	G	T		99.1%	2	0	missense	Q363K	rs772926214		2.0.E-05	2.2.E-04	none	6.0.E-04
	38,812,783	C	T		98.5%	0	1	missense	V196I			4.0.E-06	none	none	none
	38,812,804	A	G		99.3%	0	1	missense	W189R	rs1379282429		none	none	none	5.0.E-04
	38,833,581	T	G		97.5%	0	1	missense	N117H	rs774462243		6.0.E-05	8.5.E-04	none	6.0.E-04
	38,835,449	G	A		100.0%	3	1	missense	P18L	rs190176472	Benign	3.3.E-04	4.5.E-03	6.0.E-04	6.0.E-03
19	35,524,682	C	T	*SCN1B*	100.0%	0	1	missense	R163W			4.8.E-05	1.6.E-04	none	none
	35,524,755	G	A		100.0%	7	6	missense	R187H	rs72558026	Conflicting interpretations of pathogenicity	1.4.E-03	9.6.E-03	4.8.E-03	7.1.E-03
	35,524,868	C	T		100.0%	1	0	missense	R225C			1.2.E-04	none	2.0.E-04	none
	35,524,980	G	A		100.0%	0	1	missense	C262Y	rs369032304	Uncertain significance	1.6.E-04	2.2.E-03	none	1.0.E-04
	35,530,138	C	T		99.4%	0	1	missense	T189M			1.9.E-04	1.9.E-03	6.0.E-04	5.0.E-04
11	118,038,968	G	A	*SCN2B*	100.0%	0	1	missense	R94W	rs760016611		1.8.E-05	5.0.E-05	none	none
	118,038,998	G	A		100.0%	0	1	missense	R84C	rs760669515	Uncertain significance	6.4.E-05	1.6.E-04	none	4.0.E-04
11	123,513,271	C	T	*SCN3B*	100.0%	2	2	missense	V110I	rs147205617	Conflicting interpretations of pathogenicity	3.1.E-04	2.6.E-03	4.0.E-04	2.4.E-03
	123,516,452	A	G		96.6%	0	2	missense	V21A	rs749596563		1.2.E-05	1.6.E-04	none	2.1.E-03
7	83,640,592	T	G	*SEMA3A*	99.4%	0	1	missense	S278R			none	none	none	1.0.E-04
	83,643,590	C	T		98.7%	1	0	missense	E249K			none	none	none	none
3	57,743,404	C	G	*SLMAP*	97.8%	1	0	missense	T9S			none	none	none	none
	57,902,725	A	C		99.4%	1	1	missense	E727A	rs765326482		6.0.E-05	8.2.E-04	none	1.6.E-03
	57,902,737	G	A		99.4%	0	2	missense	R731Q	rs141277984		2.0.E-05	none	none	9.0.E-04
	57,908,734	G	A		98.4%	0	1	missense	R793Q	rs55766107		2.1.E-05	none	none	none
	57,913,071	G	A		97.6%	0	1	missense	A815T	rs1210310709		7.2.E-06	none	none	none
19	49,661,513	C	T	*TRPM4*	100.0%	1	1	missense	P30L	rs200868666		4.0.E-06	5.4.E-05	2.0.E-04	7.0.E-04
	49,674,674	C	T		99.9%	1	0	missense	T286M			7.2.E-05	1.1.E-04	none	none
	49,674,854	A	G		99.9%	1	0	missense	Q293R	rs172147855		1.8.E-04	1.1.E-03	8.0.E-04	5.0.E-04
	49,674,962	G	A		99.7%	1	1	missense	G329D	rs1438186663		none	none	none	4.0.E-04
	49,684,674	GA	G		99.7%	0	1	frameshift	D407AfsX27			none	none	none	2.0.E-04
	49,684,714	G	A		96.3%	1	0	nonsense	W420X	rs746740271		none	none	none	1.0.E-04
	49,685,946	C	T		100.0%	1	2	missense	R459C	rs762730503		3.2.E-05	4.4.E-04	none	2.0.E-04
	49,686,061	A	G		100.0%	0	1	missense	E497G	rs753611182		2.4.E-05	2.2.E-04	none	5.0.E-04
	49,686,103	T	A		99.4%	0	4	missense	L511Q	rs200508171	Uncertain significance	5.5.E-05	4.1.E-06	2.0.E-04	3.7.E-03
	49,691,902	C	T		100.0%	0	1	missense	S583F			none	none	none	none
	49,693,975	C	T		99.9%	1	0	missense	R719W			4.0.E-05	none	none	none
	49,699,988	C	G		97.9%	0	2	missense	S480R	rs749938388		1.1.E-04	1.4.E-03	none	8.0.E-04
	49,703,600	A	G		100.0%	1	4	missense	I897V	rs201172677		4.0.E-07	4.9.E-04	2.0.E-04	3.0.E-03
	49,705,251	CGGAGCCCGGCTTCTGGGCACACCCTCCT	C		99.4%	0	4	frameshift	L996PfsX8	rs765535147	Uncertain significance	6.0.E-05	3.0.E-04	none	1.3.E-03

*; Rare variations of other BrS-associated genes (*ABCC9, ANK2, CACNB2, KCNE5, FGF12*) were absent in cases or controls

Table S8. Gene-wise rare variant association test for non-*SCN5A* BrS-associated genes with limited or disputed evidence

BrS-associated genes		Cases (n=288)		Controls (n=372)		P-values
Non-*SCN5A* genes (n=17)*	*SCN5A*-modifying genes (n=8)	frequency	n	frequency	n	
CACNA1C		1.7%	5	3.8%	11	0.45
CACNA2D1		0.0%	0	0.3%	1	1.00
GPD1L	*GPD1L*	0.7%	2	0.0%	0	0.19
HCN4		2.8%	8	1.7%	5	0.26
KCND3		0.3%	1	0.0%	0	0.44
KCNE3		0.0%	0	0.7%	2	0.51
KCNH2		0.7%	2	0.7%	2	1.00
KCNJ8		0.0%	0	0.7%	2	0.51
PKP2	*PKP2*	2.8%	8	3.1%	9	0.81
MOG1	*MOG1*	0.0%	0	1.4%	4	0.14
SCN10A	*SCN10A*	10.4%	30	11.1%	32	0.50
SCN1B	*SCN1B*	2.8%	8	3.1%	9	0.81
SCN2B	*SCN2B*	0.0%	0	0.7%	2	0.51
SCN3B	*SCN3B*	0.7%	2	1.4%	4	0.70
SEMA3A		0.3%	1	0.3%	1	1.00
SLMAP	*SLMAP*	0.7%	2	1.7%	5	0.48
TRPM4		2.8%	8	7.3%	21	0.09
total			77		110	

Statistical analysis was performed with Fisher's exact test. *; Rare variations of other BrS-associated genes (*ABCC9, ANK2, CACNB2, KCNE5, FGF12*) were absent in cases or controls.

REFERENCES

1. Yamagata K, Horie M, Aiba T, Ogawa S, Aizawa Y, Ohe T, Yamagishi M, Makita N, Sakurada H, Tanaka T, Shimizu A, Hagiwara N, Kishi R, Nakano Y, Takagi M, Makiyama T, Ohno S, Fukuda K, Watanabe H, Morita H, Hayashi K, Kusano K, Kamakura S, Yasuda S, Ogawa H, Miyamoto Y, Kapplinger JD, Ackerman MJ, Shimizu W. Genotype-Phenotype Correlation of *SCN5A* Mutation for the Clinical and Electrocardiographic Characteristics of Probands With Brugada Syndrome: A Japanese Multicenter Registry. Circulation 2017;135:2255-2270.
2. Kapplinger JD, Giudicessi JR, Ye D, Tester DJ, Callis TE, Valdivia CR, Makielski JC, Wilde AA, Ackerman MJ. Enhanced Classification of Brugada Syndrome-Associated and Long-QT Syndrome-Associated Genetic Variants in the *SCN5A*-Encoded Na(v)1.5 Cardiac Sodium Channel. Circ Cardiovasc Genet 2015;8:582-95.
3. Genome Aggregation Database. https://gnomad.broadinstitute.org/
4. 1000 Human Genomes Project Database. https://www.internationalgenome.org/1000-genomes-browsers/
5. Integrative Japanese Genome Variation Database from Tohoku Medical Megabank (4.7KJPN). https://jmorp.megabank.tohoku.ac.jp/202001/
6. Richards S, Aziz N, Bale S, Bick D, Das S, Gastier-Foster J, Grody WW, Hegde M, Lyon E, Spector E, Voelkerding K, Rehm HL, Committee ALQA. Standards and guidelines for the interpretation of sequence variants: a joint consensus recommendation of the American College of Medical Genetics and Genomics and the Association for Molecular Pathology. Genet Med 2015;17:405-24.
7. Abe K, Machida T, Sumitomo N, Yamamoto H, Ohkubo K, Watanabe I, Makiyama T, Fukae S, Kohno M, Harrell DT, Ishikawa T, Tsuji Y, Nogami A, Watabe T, Oginosawa Y, Abe H, Maemura K, Motomura H, Makita N. Sodium channelopathy underlying familial sick sinus syndrome with early onset and predominantly male characteristics. Circ Arrhythm Electrophysiol 2014;7:511-7.
8. Itoh H, Shimizu M, Takata S, Mabuchi H, Imoto K. A novel missense mutation in the SCN5A gene associated with Brugada syndrome bidirectionally affecting blocking actions of antiarrhythmic drugs. J Cardiovasc Electrophysiol 2005;16:486-93.
9. R Core Team (2020) R: A language and environment for statistical computing. R Foundation for Statistical Computing, Vienna, Austria. http://www.r-project.org/index.html
10. Davison A, Hinkley D. Bootstrap Methods and Their Applications. Cambridge: Cambridge University Press; 1997.
11. Canty A, Ripley B. boot: Bootstrap R (S-Plus) Functions. R package version 1.3-27. 2021.
12. Therneau T (2020). A Package for Survival Analysis in R. R package version 3.2-7 https://CRAN.R-project.org/package=survival
13. Morimoto Y, Shimada-Sugimoto M, Otowa T, Yoshida S, Kinoshita A, Mishima H, Yamaguchi N, Mori T, Imamura A, Ozawa H, Kurotaki N, Ziegler C, Domschke K, Deckert J, Umekage T, Tochigi M, Kaiya H, Okazaki Y, Tokunaga K, Sasaki T, Yoshiura KI, Ono S. Whole-exome sequencing and gene-based

rare variant association tests suggest that PLA2G4E might be a risk gene for panic disorder. Transl Psychiatry 2018;8:41.

14. ExAC. https://gnomad.broadinstitute.org/
15. ESP6500. https://evs.gs.washington.edu/EVS/
16. Human Genetic Variation Database (HGVD). http://www.hgvd.genome.med.kyoto-u.ac.jp/
17. Integrative Japanese Genome Variation Database from Tohoku Medical Megabank (2KJPN). https://jmorp.megabank.tohoku.ac.jp/202001/downloads/legacy/#variant
18. GENCODE. https://www.gencodegenes.org/human/release_19.html
19. Li B, Leal SM. Methods for detecting associations with rare variants for common diseases: application to analysis of sequence data. Am J Hum Genet 2008;83:311-21.
20. Madsen BE, Browning SR. A groupwise association test for rare mutations using a weighted sum statistic. PLoS Genet 2009;5:e1000384.
21. Lee S, Wu MC, Lin X. Optimal tests for rare variant effects in sequencing association studies. Biostatistics 2012;13:762-75.
22. Efficient and Parallelizable Association Container Toolbox (EPACTS) https://github.com/statgen/EPACTS
23. Itoh H, Shimizu M, Mabuchi H, Imoto K. Clinical and electrophysiological characteristics of Brugada syndrome caused by a missense mutation in the S5-pore site of SCN5A. J Cardiovasc Electrophysiol 2005;16:378-83.
24. Takehara N, Makita N, Kawabe J, Sato N, Kawamura Y, Kitabatake A, Kikuchi K. A cardiac sodium channel mutation identified in Brugada syndrome associated with atrial standstill. J Intern Med 2004;255:137-42.
25. Rossenbacker T, Carroll SJ, Liu H, Kuiperi C, de Ravel TJ, Devriendt K, Carmeliet P, Kass RS, Heidbuchel H. Novel pore mutation in SCN5A manifests as a spectrum of phenotypes ranging from atrial flutter, conduction disease, and Brugada syndrome to sudden cardiac death. Heart Rhythm 2004;1:610-5.
26. Otagiri T, Kijima K, Osawa M, Ishii K, Makita N, Matoba R, Umetsu K, Hayasaka K. Cardiac ion channel gene mutations in sudden infant death syndrome. Pediatr Res 2008;64:482-7.
27. de la Roche J, Angsutararux P, Kempf H, Janan M, Bolesani E, Thiemann S, Wojciechowski D, Coffee M, Franke A, Schwanke K, Leffler A, Luanpitpong S, Issaragrisil S, Fischer M, Zweigerdt R. Comparing human iPSC-cardiomyocytes versus HEK293T cells unveils disease-causing effects of Brugada mutation A735V of NaV1.5 sodium channels. Sci Rep 2019;9:11173.
28. Watanabe H, Nogami A, Ohkubo K, Kawata H, Hayashi Y, Ishikawa T, Makiyama T, Nagao S, Yagihara N, Takehara N, Kawamura Y, Sato A, Okamura K, Hosaka Y, Sato M, Fukae S, Chinushi M, Oda H, Okabe M, Kimura A, Maemura K, Watanabe I, Kamakura S, Horie M, Aizawa Y, Shimizu W, Makita N. Electrocardiographic characteristics and SCN5A mutations in idiopathic ventricular fibrillation associated with early repolarization. Circ Arrhythm Electrophysiol 2011;4:874-81.
29. Zhang Y, Wang T, Ma A, Zhou X, Gui J, Wan H, Shi R, Huang C, Grace AA, Huang CL, Trump D,

Zhang H, Zimmer T, Lei M. Correlations between clinical and physiological consequences of the novel mutation R878C in a highly conserved pore residue in the cardiac Na+ channel. Acta Physiol (Oxf) 2008;194:311-23.

30. Medeiros-Domingo A, Tan BH, Iturralde-Torres P, Tester DJ, Tusie-Luna T, Makielski JC, Ackerman MJ. Unique mixed phenotype and unexpected functional effect revealed by novel compound heterozygosity mutations involving SCN5A. Heart Rhythm 2009;6:1170-5.
31. Turker I, Makiyama T, Vatta M, Itoh H, Ueyama T, Shimizu A, Ai T, Horie M. A Novel SCN5A Mutation Associated with Drug Induced Brugada Type ECG. PLoS One 2016;11:e0161872.
32. Kyndt F, Probst V, Potet F, Demolombe S, Chevallier JC, Baro I, Moisan JP, Boisseau P, Schott JJ, Escande D, Le Marec H. Novel SCN5A mutation leading either to isolated cardiac conduction defect or Brugada syndrome in a large French family. Circulation 2001;104:3081-6.
33. Zhu JF, Du LL, Tian Y, Du YM, Zhang L, Zhou T, Tian LI. Novel heterozygous mutation c.4282G>T in the SCN5A gene in a family with Brugada syndrome. Exp Ther Med 2015;9:1639-1645.
34. Frustaci A, Priori SG, Pieroni M, Chimenti C, Napolitano C, Rivolta I, Sanna T, Bellocci F, Russo MA. Cardiac histological substrate in patients with clinical phenotype of Brugada syndrome. Circulation 2005;112:3680-7.
35. Wang DW, Yazawa K, George AL, Jr., Bennett PB. Characterization of human cardiac Na+ channel mutations in the congenital long QT syndrome. Proc Natl Acad Sci U S A 1996;93:13200-5.
36. Valdivia CR, Tester DJ, Rok BA, Porter CB, Munger TM, Jahangir A, Makielski JC, Ackerman MJ. A trafficking defective, Brugada syndrome-causing SCN5A mutation rescued by drugs. Cardiovasc Res 2004;62:53-62.
37. Makita N, Behr E, Shimizu W, Horie M, Sunami A, Crotti L, Schulze-Bahr E, Fukuhara S, Mochizuki N, Makiyama T, Itoh H, Christiansen M, McKeown P, Miyamoto K, Kamakura S, Tsutsui H, Schwartz PJ, George AL, Jr., Roden DM. The E1784K mutation in *SCN5A* is associated with mixed clinical phenotype of type 3 long QT syndrome. J Clin Invest 2008;118:2219-29.
38. Yang Z, Lu D, Zhang L, Hu J, Nie Z, Xie C, Qiu F, Cheng H, Yan Y. p.N1380del mutation in the pore-forming region of SCN5A gene is associated with cardiac conduction disturbance and ventricular tachycardia. Acta Biochim Biophys Sin (Shanghai) 2017;49:270-276.
39. Makita N, Sumitomo N, Watanabe I, Tsutsui H. Novel SCN5A mutation (Q55X) associated with age-dependent expression of Brugada syndrome presenting as neurally mediated syncope. Heart Rhythm 2007;4:516-9.
40. Kawamura M, Ozawa T, Yao T, Ashihara T, Sugimoto Y, Yagi T, Itoh H, Ito M, Makiyama T, Horie M. Dynamic change in ST-segment and spontaneous occurrence of ventricular fibrillation in Brugada syndrome with a novel nonsense mutation in the SCN5A gene during long-term follow-up. Circ J 2009;73:584-8.
41. Makiyama T, Shizuta S, Akao M, Kimura T, Horie M. Genetic Background of Arrhythmic Disorders. Jpn. J. Electrocardiol 2010;30:200-208.
42. Benson DW, Wang DW, Dyment M, Knilans TK, Fish FA, Strieper MJ, Rhodes TH, George AL, Jr.

Congenital sick sinus syndrome caused by recessive mutations in the cardiac sodium channel gene (SCN5A). J Clin Invest 2003;112:1019-28.